



Cite this: *Food Funct.*, 2021, **12**, 6558

## Gut microbiota mediates the effects of curcumin on enhancing Ucp1-dependent thermogenesis and improving high-fat diet-induced obesity†

Zaiqi Han, <sup>a</sup> Lu Yao, <sup>b,c</sup> Yue Zhong, <sup>d,e</sup> Yang Xiao, <sup>a</sup> Jing Gao, <sup>a</sup> Zhaozheng Zheng, <sup>a</sup> Sijia Fan, <sup>a</sup> Ziheng Zhang, <sup>a</sup> Shanggang Gong, <sup>a</sup> Sheng Chang, <sup>a</sup> Xiaona Cui<sup>f,g</sup> and Jianhui Cai<sup>\*h</sup>

Due to extremely poor systemic bioavailability, the mechanism by which curcumin increases energy expenditure remains unelucidated. Accumulating evidence suggests a strong association between the gut microbiota (GM) and energy metabolism. We investigated whether the GM mediates the effects of curcumin on improving energy homeostasis. High-fat diet (HFD)-fed wild type, uncoupling protein 1 (Ucp1) knockout and G protein-coupled membrane receptor 5 (TGR5) knockout mice were treated with curcumin ( $100 \text{ mg kg}^{-1} \text{ d}^{-1}$ , p.o.). Curcumin-treated HFD-fed mice displayed decreased body weight gain and augmented cold tolerance due to enhanced adaptive thermogenesis as compared with that in control mice. The anti-obesity effects of curcumin were abolished by Ucp1 knockout. 16S ribosomal DNA sequencing analysis revealed that curcumin restructured the GM in HFD-fed mice. Fecal microbiota transplantation (FMT) and endogenous GM depletion indicated that the GM mediated the enhanced effect of curcumin on Ucp1-dependent thermogenesis. Curcumin altered bile acid (BA) metabolism with increased fractions of circulating deoxycholic acid (DCA) and lithocholic acid (LCA), which are the two most potent ligands for TGR5. Consistently, the enhanced effect of curcumin on Ucp1-dependent thermogenesis was eliminated by TGR5 knockout. Curcumin requires the GM and TGR5 to activate the cyclic adenosine monophosphate (cAMP)/protein kinase A (PKA) signaling pathway in thermogenic adipose tissue. Here, we demonstrated that the GM mediates the effects of curcumin on enhancing Ucp1-dependent thermogenesis and ameliorating HFD-induced obesity by influencing BA metabolism. We disclosed the potential of nutritional and pharmacologic manipulations of the GM to enhance Ucp1-dependent thermogenesis in the prevention and treatment of obesity.

Received 10th March 2021,  
Accepted 1st June 2021

DOI: 10.1039/d1fo00671a  
[rsc.li/food-function](http://rsc.li/food-function)

<sup>a</sup>College of Pharmacy, Jilin Medical University, Jilin, Jilin, China  
<sup>b</sup>College of Basic Medical Sciences, Jilin Medical University, Jilin, Jilin, China.  
E-mail: [y1228@aliyun.com](mailto:y1228@aliyun.com)

<sup>c</sup>Experimental Center of Research on Prevention and Treatment of Chronic Diseases, Jilin Medical University, Jilin, Jilin, China

<sup>d</sup>Department of Biochemistry and Molecular Biology, School of Basic Medical Sciences, Xi'an Jiaotong University Health Science Center, Xi'an, Shanxi, China

<sup>e</sup>College of management, Jilin Medical University, Jilin, Jilin, China

<sup>f</sup>Department of Endocrinology and Metabolism, Peking University Third Hospital, Beijing, China

<sup>g</sup>Clinical Stem Cell Research Center, Peking University Third Hospital, Beijing, China  
<sup>h</sup>Jilin Collaborative Innovation Center for Antibody Engineering, Jilin Medical University, Jilin Jilin, China. E-mail: [jianhucuai@aliyun.com](mailto:jianhucuai@aliyun.com)

† Electronic supplementary information (ESI) available. See DOI: [10.1039/d1fo00671a](https://doi.org/10.1039/d1fo00671a)

‡ These authors contributed equally to this work.

## Introduction

A sedentary lifestyle and calorie-rich diet have rendered obesity a worldwide epidemic.<sup>1</sup> However, treatments to deal with obesity are limited.<sup>2</sup> Non-shivering thermogenesis can dissipate energy to generate heat and, hence, have an anti-obesity effect. Studies have indicated two types of non-shivering thermogenesis, Ucp1-dependent and Ucp1-independent.<sup>3,4</sup> Ucp1-dependent thermogenesis dissipates the mitochondrial proton gradient to generate heat instead of synthesizing ATP through uncoupling of respiration in brown and beige adipose cells, whereas Ucp1-independent thermogenesis generates heat in the absence of Ucp1.<sup>4</sup> Adult humans possess UCP1-positive cells in adipose tissue, so increasing the Ucp1-dependent thermogenesis of adipose tissue in humans may represent an attractive strategy for preventing and even curing obesity.<sup>5,6</sup> However, a clinically safe and available method to induce Ucp1-dependent thermogenesis in humans is not

known. Thus, the discovery of a novel therapeutic approach to combat obesity by enhancing Ucp1-dependent thermogenesis is imperative.

Curcumin is derived from the tropical plant *Curcuma longa*. It has been used as a dietary agent, food preservative and traditional Asian medicine for many years.<sup>7</sup> Recently, several studies have shown dietary curcumin to promote the expression of Ucp1 in brown adipose tissue (BAT) and browning of white adipose tissue (WAT), thereby increasing energy expenditure and preventing obesity.<sup>8,9</sup> However, the precise contribution of Ucp1-dependent thermogenesis in the anti-obesity effects of curcumin has not yet been evaluated critically. Moreover, orally administered curcumin is barely released into the circulation due to extremely poor systemic bioavailability.<sup>10,11</sup> Therefore, it is reasonable to infer that the gastrointestinal tract is the organ where curcumin helps to improve energy homeostasis. Based on those observations, further studies are needed to understand the mechanism by which curcumin possesses anti-obesity activity, thereby providing additional therapeutic agents to prevent obesity.

Emerging evidence suggests a strong association between the gut microbiota (GM) and obesity, thereby hinting at the GM being an important environmental factor involved in energy metabolism.<sup>12,13</sup> Up to one-third of the metabolites found in mammalian blood are estimated to be derived from the GM.<sup>12</sup> Bile acids (BAs) belong to a class of such metabolites. They are produced in the liver, and are biochemically modified by gut bacteria.<sup>14</sup> Primary BAs are synthesized from cholesterol through the classical pathway or alternative pathway in the liver, and expelled into the intestine to aid the digestion and absorption of lipids and fat-soluble vitamins.<sup>15</sup> Apart from being reabsorbed in the terminal ileum and recycled by the host, primary BAs can be converted to secondary BAs by the GM in the colon through deconjugation, dehydrogenation, dihydroxylation, and isomerization.<sup>16</sup> Besides their role in BA biotransformation, the GM can also influence hepatic BA synthesis by regulating the expression of key enzymes involved in BA synthesis.<sup>14,17</sup> BAs can function as signaling molecules for many tissues and influence host metabolism through BA-sensing receptor-mediated signal pathways.<sup>15</sup> Among them, BAs have been found to increase the activity of BAT *via* G protein-coupled bile acid receptor 5 (TGR5).<sup>18</sup> The latter is activated predominately by the secondary BAs lithocholic acid (LCA) and deoxycholic acid (DCA). TGR5 is expressed widely in many tissues, including BAT and WAT.<sup>14</sup> TGR5 activation induces mitochondrial uncoupling and oxygen consumption through upregulation of cyclic adenosine monophosphate (cAMP) production and the cAMP/protein kinase A (PKA) signaling pathway.<sup>19</sup> Overall, activation of the TGR5 signaling pathway in thermogenic adipose tissue *via* the GM may represent a promising avenue for improving energy homeostasis and combating obesity.

We investigated the effects of oral administration of curcumin on the GM, BA metabolism and thermogenic adipose tissue. Ucp1 knockout (*Ucp1*<sup>-/-</sup>) mice were used to evaluate the contribution of Ucp1-dependent thermogenesis in the

anti-obesity effects of curcumin. Furthermore, experiments on fecal microbiota transplantation (FMT) and depletion of endogenous GM were employed to clarify the role of the GM in the effects of curcumin on improving energy homeostasis. TGR5 knockout (*Gphar1*<sup>-/-</sup>) mice were employed to ascertain the mechanism by which curcumin enhanced Ucp1-dependent thermogenesis. We aimed to explore the potential role and mechanisms of the GM in the effects of curcumin on ameliorating HFD-induced obesity. This knowledge may disclose the potential of nutritional and pharmacologic manipulations of the GM to enhance Ucp1-dependent thermogenesis in the prevention and cure of obesity.

## Materials & methods

### Ethical approval of the study protocol

All animal procedures were performed in accordance with the Guidelines for Care and Use of Laboratory Animals published by the Institute of Laboratory Animal, United States National Institute of Health (NIH Publication No. 85-23, 1996). Animal experiments were undertaken according to protocols approved by the Animal Research Committee of Jilin Medical University (Animal application approval number 2018-004, Jilin, China).

### Reagents

Curcumin (purity ≥95.0%) was purchased from Shanghai Yuanye Biotech (Shanghai, China). Carboxymethylcellulose sodium was obtained from Sigma-Aldrich (Saint Louis, MO, USA). Lipopolysaccharide (LPS) commercial kits (catalog number: CG1500) were purchased from Associates of CAPE COD (Falmouth, MA, USA). cAMP enzyme-linked immunosorbent assay (ELISA) kits (ab133051) were obtained from Abcam (Cambridge, UK). Neomycin, streptomycin, penicillin, vancomycin, metronidazole, bacitracin, ciprofloxacin, ceftazidime and gentamycin were purchased from Sangon Biotech (Shanghai, China). TRIzol® Reagent was from Invitrogen (Carlsbad, CA, USA). High-Capacity cDNA Reverse-Transcription Kits were purchased from Applied Biosystems (Foster City, CA, USA). SYBR Green PCR Master Mix was obtained from Promega (Fitchburg, MI, USA). Proteinase inhibitor cocktail and phosphorylase inhibitor were purchased from Roche (Basel, Switzerland). Bicinchoninic acid (BCA) Protein Assay Kits were purchased from Genstar Technologies (Beijing, China). Antibodies against Ucp1 (ab10983), TGR5 (ab72608) and cytochrome P450, family 8, subfamily b, polypeptide 1 (Cyp8b1; ab191910) were purchased from Abcam. The antibody against cytochrome P450, family 7, subfamily a, polypeptide 1 (Cyp7a1; PA5-100892) was obtained from Invitrogen. The antibody against cytochrome P450, family 7, subfamily b, polypeptide 1 (Cyp7b1; 24889-2-AP) was purchased from Proteintech (Beijing, China). The antibody against Tubulin (CW0098) was from CwbioTech (Beijing, China). Antibodies against cAMP-responsive element-binding protein (Creb; 9197) and phosphorylated Creb (pCreb; 9198) were purchased from Cell Signaling Technology (Danvers, MA, USA).

## Animals

Specific pathogen-free (SPF) 8-week-old male C57BL/6J mice purchased from Charles River Laboratories (Beijing, China), *Ucp1*<sup>-/-</sup> mice obtained from Jackson Laboratory (bar Harbor, ME, USA) and *Gpbar1*<sup>-/-</sup> mice purchased from Bioray Laboratory (Shanghai, China) were housed and maintained under a 12 h light/dark photoperiod at a constant temperature (23 °C) with unlimited availability of water and food. Two types of knockout mice were backcrossed with C57BL/6J mice for >8 generations. Mice were fed a HFD (D12492; Research Diets, New Brunswick, NJ, USA) to induce obesity. Mice possessing an identical genotype were grouped randomly into two groups. Curcumin dissolved in 0.5% carboxymethylcellulose was administered to mice daily by intragastric gavage since mice were fed with HFD or 8-week-old; 0.5% carboxymethylcellulose sodium was administered to the vehicle group as controls. Preliminary experimental results showed that curcumin could not significantly prevent HFD-induced obesity until the gavage dose was as high as 100 mg per kg bodyweight (data not shown). Therefore, we chose 100 mg per kg bodyweight as the gavage dose of curcumin.

To deplete endogenous GM from C57BL/6J mice after 4 weeks of treatment with curcumin or vehicle during HFD feeding, antibiotics were administered *via* drinking water, and replaced with freshly prepared antibiotics every second day for 4 weeks. The antibiotics regimen was neomycin (100 µg mL<sup>-1</sup>), streptomycin (50 µg mL<sup>-1</sup>), penicillin (100 U mL<sup>-1</sup>), vancomycin (50 µg mL<sup>-1</sup>), metronidazole (100 µg mL<sup>-1</sup>), bacitracin (1 mg mL<sup>-1</sup>), ciprofloxacin (125 µg mL<sup>-1</sup>), ceftazidime (100 µg mL<sup>-1</sup>), and gentamycin (170 µg mL<sup>-1</sup>). Meanwhile, antibiotics-treated mice were administered curcumin or vehicle, as appropriate, every day.

SPF 4-week-old male C57BL/6J mice were used to generate endogenous GM-depleted recipient mice. FMT was undertaken based on an established protocol.<sup>13</sup> Briefly, 500 mg of fresh feces from curcumin-treated or vehicle-treated HFD-fed mice was resuspended in 5 mL of sterile reduced phosphate-buffered saline. The suspension was allowed to settle by gravity for 5 min, after which a 200 µL aliquot of supernatant was administrated to recipient mice by intragastric gavage. All recipient mice were fed a HFD, and FMT was carried out daily. Fresh transplant materials were prepared on the same day of transplantation, <10 min before gavage, to prevent changes in bacterial composition.

For all experiments in this study, male, age- and genotype-matched mice using the corresponding treatment were used. In addition to experiments on acute exposure to cold without fasting, all mice went through a 6 h fast under deep isoflurane-induced anesthesia before blood was collected from the inferior vena cava, and tissues were harvested for further analyses.

## Measurement of bodyweight, food intake and energy expenditure

Bodyweight and food intake were measured weekly. For metabolic studies, mice were housed individually in metabolic

cages (Panlab/Harvard apparatus; Cornellà, Barcelona, Spain) and had free access to food and water. The rate of oxygen consumption was monitored for 24 h. Activity monitoring was done simultaneously with metabolic measurements.

## Histology

For hematoxylin & eosin (H&E) staining, BAT, inguinal white adipose tissue (iWAT), epididymal white adipose tissue (eWAT), liver, small intestine and colon tissues were fixed in 10% neutral-buffered formalin, embedded in paraffin, and cut into sections of thickness 7 µm. Then the sections were stained with H&E. For transmission electron microscopy, BAT and iWAT were fixed with 2.5% glutaraldehyde (pH 7.4) overnight at 4 °C, and then postfixed with 2% osmium tetroxide for 1 h at room temperature. Thin sections were stained with uranyl acetate and lead citrate, and examined with a JEM-1010 electron microscope (Jeol, Tokyo, Japan). Representative images were repeated in at least three independent experiments. The size of adipose cells was measured in H&E-stained sections of at least three individual samples in each group. The average diameter of adipocyte cells was analyzed using ImageJ (National Institutes of Health, Bethesda, MD, USA).

## Output of fecal energy

Bomb calorimetry was undertaken on fecal samples collected from mice to measure fecal caloric content, as described previously.<sup>20</sup> Fecal samples were collected, and oven dried for 48 h at 58 °C. Gross energy content was measured using an isoperibol bomb calorimeter (C 2000; IKA Works, Wilmington, MA, USA). The energy equivalent factor of the calorimeter was determined using a standard (benzoic acid).

## Biochemical analyses

Serum concentrations of aspartate aminotransferase (AST) and alanine transaminase (ALT) were determined using an automated Monarch® device (Instrumentation Laboratory, Lexington, MA, USA) at the clinical laboratory of Jilin 465 Hospital (Jilin, China).

## Acute exposure to cold

For experiments on acute exposure to cold, mice were placed in a fridge (4 °C) with free access to food and water. The core body temperature was monitored using a rectal probe (ThermoWorks, Alpine, UT, USA). After cold exposure for 6 h, BAT and iWAT were harvested from deep isoflurane-induced anesthetized mice for further analyses.

## Infrared thermography

The body temperature of mice was recorded with an infrared camera (FLIR Tools™; Wilsonville, OR, USA) and analyzed with FLIR Tools. For each animal/group, at least five pictures were taken and analyzed.

## Quantitative real-time PCR

Total RNA was extracted from tissues with TRIzol Reagent according to manufacturer instructions. For quantitative real-

time PCR analysis, 2 µg of total RNA was reverse-transcribed using the High-Capacity cDNA Reverse-Transcription kit. SYBR Green reactions using SYBR Green PCR Master Mix were assembled along with 500 nM primers according to manufacturer instructions and undertaken with a C1000 Thermal Cycler CFX96 Real-Time system (Bio-Rad Laboratories, Hercules, CA, USA) or an ABI 7500-Fast Real-Time PCR system (Applied Biosystems). Relative expression of mRNAs was determined after normalization to ribosomal protein S18 (*Rps18*). Primer sequences are shown in ESI Table 1.†

### Protein extraction and western blotting

Tissue lysates were prepared using RIPA buffer supplemented with a proteinase inhibitor cocktail, phenylmethylsulfonyl fluoride and phosphorylase inhibitor. Protein concentrations were determined using the BCA Protein Assay Kit. Protein from the indicated samples was separated by sodium dodecyl sulfate-polyacrylamide gel electrophoresis and transferred onto polyvinylidene difluoride membranes. The latter were incubated with the respective polyclonal antibodies. After washing, horseradish peroxidase-conjugated anti-rabbit immunoglobulin (Ig)G and anti-mouse IgG were used as the secondary antibody at 1:5000 dilution. Relative protein images were determined using horseradish peroxidase-conjugated secondary antibodies and electrochemiluminescence substrates. The intensities of the immunoreactive bands were quantified by densitometry using Image Lab (Bio-Rad Laboratories).

### GM analyses

The genomic DNA of fecal samples was extracted by the FastDNA® SPIN Kit for Soil (MP Biomedicals, Santa Ana, CA, USA) according to manufacturer instructions. The quantity and quality of extracted DNA were assessed by agarose gel electrophoresis and spectrophotometry (NanoDrop™ 2000, Thermo Scientific, Waltham, MA, USA). The V3–V4 region of bacterial 16S ribosome of each stool sample was amplified by PCR using a forward primer (5'-CCT ACG GGN GGC WGC AG-3') and reverse primer (5'-GAC TAC HVG GGT ATC TAA TCC-3'). The sequencing and bioinformatics analysis of fecal samples were done on the MiSeq® Benchtop Sequencer (Illumina, San Diego, CA, USA) by Genesky Biotechnology (Beijing, China). High-quality sequence clustering was carried out by the UPARSE algorithm based on the Ribosomal Database Project (<https://rdp.cme.msu.edu/index.jsp>) and clustered into operational taxonomic units with a similarity cutoff of 97%. Beta diversity analysis was undertaken to investigate the structural variation of microbial communities across samples using weighted UniFrac distance metrics and visualized via principal coordinate analysis (PCoA). The significance for PCoA analyses was obtained via the R package (R Institute for Statistical Computing, Vienna, Austria) ADONIS, which is a permutational multivariate analysis of variance that is designed for distance matrices. Samples were hierarchical-clustered with the unweighted pair group method with arithmetic mean method based on the Bray–Curtis distance matrix.

A statistical method introduced in Metastats (<http://metastats.cbcn.umd.edu/detection.html>) was used to reveal significant differences of microbial communities between curcumin-treated and vehicle-treated HFD-fed mice. Linear discriminant analysis (LDA) scores derived from linear discriminant analysis effect size (LEfSe) studies, showed the biomarker taxa (LDA score >2 and significance  $P < 0.05$  determined by the nonparametric Wilcoxon sum-rank test). The raw data for sequencing generated in our study have been deposited in the Genome Sequence Archive in the Big Data Center in the Beijing Institute of Genomics within the Chinese Academy of Sciences (Shanghai, China) under accession number CRA004001, and are accessible at <https://bigd.big.ac.cn/gsa>.

With regard to the fecal samples obtained from endogenous GM-depleted mice colonized with microbiota from vehicle- or curcumin-treated HFD-fed mice, genomic DNA were extracted by a soil/fecal DNA extraction kit (Tianmo Biotech, Beijing, China). The quantity and quality of extracted DNA were assessed with agarose-gel electrophoresis and spectrophotometry (NanoDrop™ 2000; Thermo Scientific) and then real-time RT-qPCR was carried out. Primer sequences have been described previously,<sup>21–24</sup> but are shown in ESI Table 1.†

### Analysis of BA composition in serum

Measurement of BA composition in serum was undertaken as reported previously.<sup>25</sup> Briefly, 50 µL of each sample was mixed with 60 µL of a methanol–water mixture (2:1, v/v) containing an internal standard and 490 µL of pre-cooled methanol for protein precipitation. Samples were centrifuged at 12 000 rpm for 10 min at 4 °C. Then, the supernatant was evaporated to dryness and redissolved in 50 µL of methanol–water (2:1, v/v) containing 0.005% HCOOH. Next, the solution was passed through a 0.22 µm membrane filter before ultra-performance liquid chromatography tandem mass-spectrometry (UPLC-MS/MS). The UPLC-MS/MS system consisted of a UPLC system (1290 series; Agilent Technologies, Santa Clara, CA, USA) coupled to a triple quadrupole mass spectrometer (6470 series; Agilent Technologies) equipped with an electrospray ionization source (Agilent Technologies). 1 µL of the extraction was injected on a ZORBAX Eclipse™ Plus C18 column (2.1 × 100 mm, 1.8 µm particles; Agilent Technologies) using a flow rate of 0.6 mL min<sup>-1</sup> at 45 °C during a 16 min gradient (0–7 min from 26% B to 32% B, 7–12 min from 32% B to 70% B, 12–13 min from 70% B to 95% B, 13–16 min 95% B), while using the solvents A (water containing 0.005% formic acid) and solvents B (acetonitrile containing 0.005% formic acid). Multiple reaction monitoring was used to qualify the fragment ions screened. The quantification was done against area of structurally similar internal standards using MassHunter™ Workstation vB.08.00 (Agilent Technologies).

### cAMP immunoassay

BAT and iWAT samples were homogenized in 0.1 M HCl and then centrifuged. After centrifugation, the supernatants were used to analyze intracellular levels of cAMP by the cAMP ELISA kit according to manufacturer instructions.

## Quantification of mitochondrial (mt)DNA copy number

Total DNA was isolated from BAT and iWAT after digestion with proteinase K ( $100\text{ }\mu\text{g mL}^{-1}$ ) by phenol/chloroform extraction. mtDNA was amplified using primers specific for mitochondrial COX2 and normalized to genomic DNA by amplification of nuclear *Rps18*. The primer sequences, which have been described previously,<sup>26</sup> are shown in ESI Table 1.<sup>†</sup>

## Statistical analyses

Numerical data are presented as the mean  $\pm$  SEM. Statistical analyses were carried out using SPSS 20 (IBM, Armonk, NY, USA).  $P < 0.05$  was considered significant and determined by two-tailed Student's *t* tests (for comparison of two experimental conditions) or ANOVA (for comparison of more than two experimental conditions) followed by Bonferroni's test. The number of animals used for each experiment is indicated in the respective figure legends.

## Results

### Curcumin ameliorates HFD-induced obesity by enhancing adaptive thermogenesis

We wished to determine the metabolic effects of curcumin. Hence, 8-week-old male C57BL/6J mice were subjected to daily curcumin treatment by intragastric gavage. On a chow diet, curcumin-treated mice were indistinguishable from vehicle-treated mice in terms of bodyweight (Fig. 1a). In contrast, on a HFD, curcumin-treated mice showed less gain in bodyweight, with no sign of hepatic or intestinal toxicity (Fig. 1b, c and ESI Fig. 1a-d<sup>†</sup>). To determine the cause underlying the decreased gain in bodyweight of curcumin-treated HFD-fed mice, different organs and fat pads (including BAT, iWAT, and eWAT) were weighed. Curcumin did not affect the weight of the kidneys, heart, and spleen (data not shown). However, the individual fat pads and liver of vehicle-treated HFD-fed mice were larger and heavier than those of curcumin-treated HFD-fed mice (Fig. 1d and e). Moreover, histology revealed curcumin to reduce the accumulation of lipid vesicles with the appearance of smaller, multilocular beige adipocytes in iWAT of curcumin-treated HFD-fed mice (Fig. 1f and g).

Key elements involved in energy homeostasis were investigated to elucidate the potential mechanism by which curcumin alleviated HFD-induced obesity. Curcumin had no effect on food intake or fecal energy loss (ESI Fig. 2a and b<sup>†</sup>). In addition, gas exchange and activity levels were monitored by housing body weight-matched curcumin- and vehicle-treated HFD-fed mice in metabolic cages. Curcumin had no influence on locomotor activity (ESI Fig. 2c<sup>†</sup>). However, curcumin caused HFD-fed mice to have consistently higher rate of oxygen consumption and carbon dioxide production compared with those in vehicle-treated HFD-fed mice (Fig. 1h and i). Furthermore, curcumin-treated HFD-fed mice displayed a lower respiration exchange ratio (RER), which implied a tendency of using lipids as an energy source (ESI Fig. 2d<sup>†</sup>). Consistent with increased energy expenditure, curcumin treat-

ment increased the core body temperature in HFD-fed mice at room temperature (Fig. 1j). Taken together, these data implied that increased adaptive thermogenesis contributed to the effects of curcumin on ameliorating HFD-induced obesity.

### Curcumin requires Ucp1 to attenuate HFD-induced obesity

During acute exposure to cold, Ucp1-dependent thermogenesis is predominately enhanced to maintain body temperature.<sup>27</sup> Upon acute exposure to cold (4 °C), curcumin-treated HFD-fed mice displayed a slowdown in the decrease of core body temperature (Fig. 2a). Thermal images revealed the higher surface temperature of curcumin-treated HFD-fed mice (Fig. 2b). Consistently, expression of thermogenic genes induced by cold stress in BAT and iWAT was intensified due to curcumin treatment (Fig. 2c-f). These results implied that curcumin increased energy expenditure by enhancing Ucp1-dependent thermogenesis. Hence, Ucp1 knockout mice could be used as a useful model to investigate the contribution of Ucp1-dependent thermogenesis to the therapeutic effects on obesity, *Ucp1*<sup>-/-</sup> mice were used to evaluate the contribution of Ucp1-dependent thermogenesis to the effects of curcumin on attenuating HFD-induced obesity.<sup>28,29</sup> We demonstrated that Ucp1 protein was not detectable in the BAT or iWAT of *Ucp1*<sup>-/-</sup> mice (Fig. 2g). *Ucp1*<sup>-/-</sup> mice utilize alternative Ucp1-independent thermogenesis to resist thermal stress at 23 °C, so *Ucp1*<sup>-/-</sup> mice usually need a longer time than wild type mice to become obese during HFD feeding.<sup>27,30</sup> Accordingly, we measured the bodyweight of curcumin- and vehicle-treated HFD-fed *Ucp1*<sup>-/-</sup> mice for 18 weeks rather than 12 weeks. Curcumin-treated HFD-fed *Ucp1*<sup>-/-</sup> mice showed similar body weight gain as vehicle-treated HFD-fed *Ucp1*<sup>-/-</sup> mice, and *Ucp1*<sup>-/-</sup> mice from the two groups were all obese after feeding with a HFD for 18 weeks (Fig. 2h and i). Moreover, the results for the organ coefficient and histology indicated no difference between these mice (ESI Fig. 3a-c<sup>†</sup>). Furthermore, curcumin treatment had no effect on the core body temperature (Fig. 2j). Consistently, thermal imaging showed the comparable surface temperature of these mice (Fig. 2k). Collectively, these data demonstrated that Ucp1 knockout eliminated the anti-obesity effects of curcumin, thereby indicating that curcumin is reliant on Ucp1 to alleviate HFD-induced obesity.

### Curcumin restructures the GM community in HFD-fed mice

To explore whether curcumin has regulatory effects on the gut microbiota, fecal microbiota was profiled by 16S ribosomal DNA-sequencing. Weighted UniFrac distance-based PCoA revealed distinct clustering of intestinal microbial communities between curcumin- and vehicle-treated HFD-fed mice (Fig. 3a). At the taxonomic level, hierarchical clustering analysis revealed a significant separation between microbiota from curcumin- and vehicle-treated HFD-fed mice (Fig. 3b). Analysis at the phylum level indicated that curcumin treatment significantly decreased the relative abundance of Bacteroidetes while increasing the relative abundance of Verrucomicrobia and Deffribacteres (Fig. 3c). To further elucidate the differences across the two groups, family- and genus-level analyses were

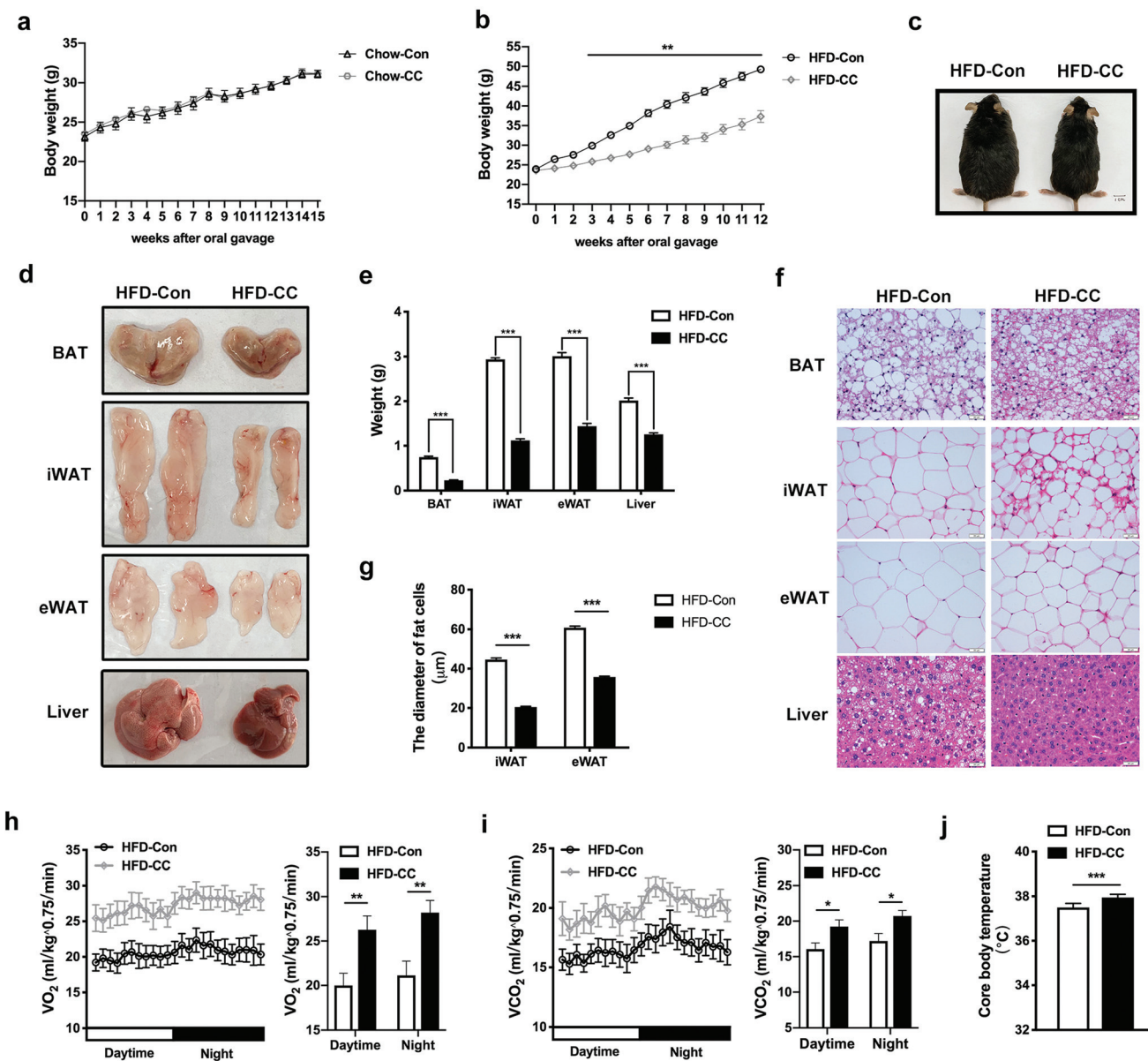


**Fig. 1** Oral administration of curcumin ameliorates HFD-induced obesity by enhancing adaptive thermogenesis. (a, b) Bodyweight gain of curcumin-treated or vehicle-treated mice during chow diet (a) and HFD (b) feeding ( $n = 8$  or 9 per group). (c) A representative photograph of HFD-fed mice treated with curcumin or vehicle for 12 weeks. (d) Representative images of BAT, iWAT, eWAT and liver from mice in (c). (e) The weight of BAT, iWAT, eWAT and liver from HFD-fed mice treated with curcumin or vehicle for 12 weeks ( $n = 8$  per group). (f) H&E staining of BAT, iWAT, eWAT and liver from mice in (e). Scale bar, 20  $\mu\text{m}$ . (g) Average diameters of fat cells from mice in (e). (h) Rate of  $\text{O}_2$  consumption (left panel), and average rate of  $\text{O}_2$  consumption (right panel) of bodyweight-matched HFD-fed mice treated with curcumin or vehicle for 3 weeks ( $n = 8$  per group). (i) Rate of  $\text{CO}_2$  production (left panel), and average rate of  $\text{CO}_2$  production (right panel) of mice in (h) ( $n = 8$  per group). (j) Rectal temperature of HFD-fed mice treated with curcumin or vehicle for 8 weeks at room temperature ( $n = 8$  per group). Numerical data are shown as the mean  $\pm$  SEM. \* $P < 0.05$ , \*\* $P < 0.01$ , \*\*\* $P < 0.001$ .

undertaken, and showed results similar to those obtained at the phylum level (Fig. 3d and e). LEFSe indicated an enriched and reduced relative abundance of *Akkermansia* and *Alistipes*, respectively, in curcumin-treated HFD-fed mice than in control mice (Fig. 3f). Intriguingly, curcumin treatment increased the relative abundance of *Lactobacillus* the prominent BSH activity-positive bacteria involved in BA metabolism and *Clostridium* cluster XIVa which can convert primary BAs to the secondary

BAs DCA and LCA, whereas it reduced the relative abundance of *Acetatifactor* bile salt-induced anaerobic bacteria.<sup>14,31,32</sup> GM dysbiosis in HFD-fed mice is associated with increased gut permeability and release of LPS into the circulation.<sup>33</sup> We examined the expression of genes involved in mucosal defense, and curcumin induced the expression of these genes (Fig. 3g). Consistently, curcumin-treated HFD-fed mice showed decreased circulating LPS concentrations (Fig. 3h). These

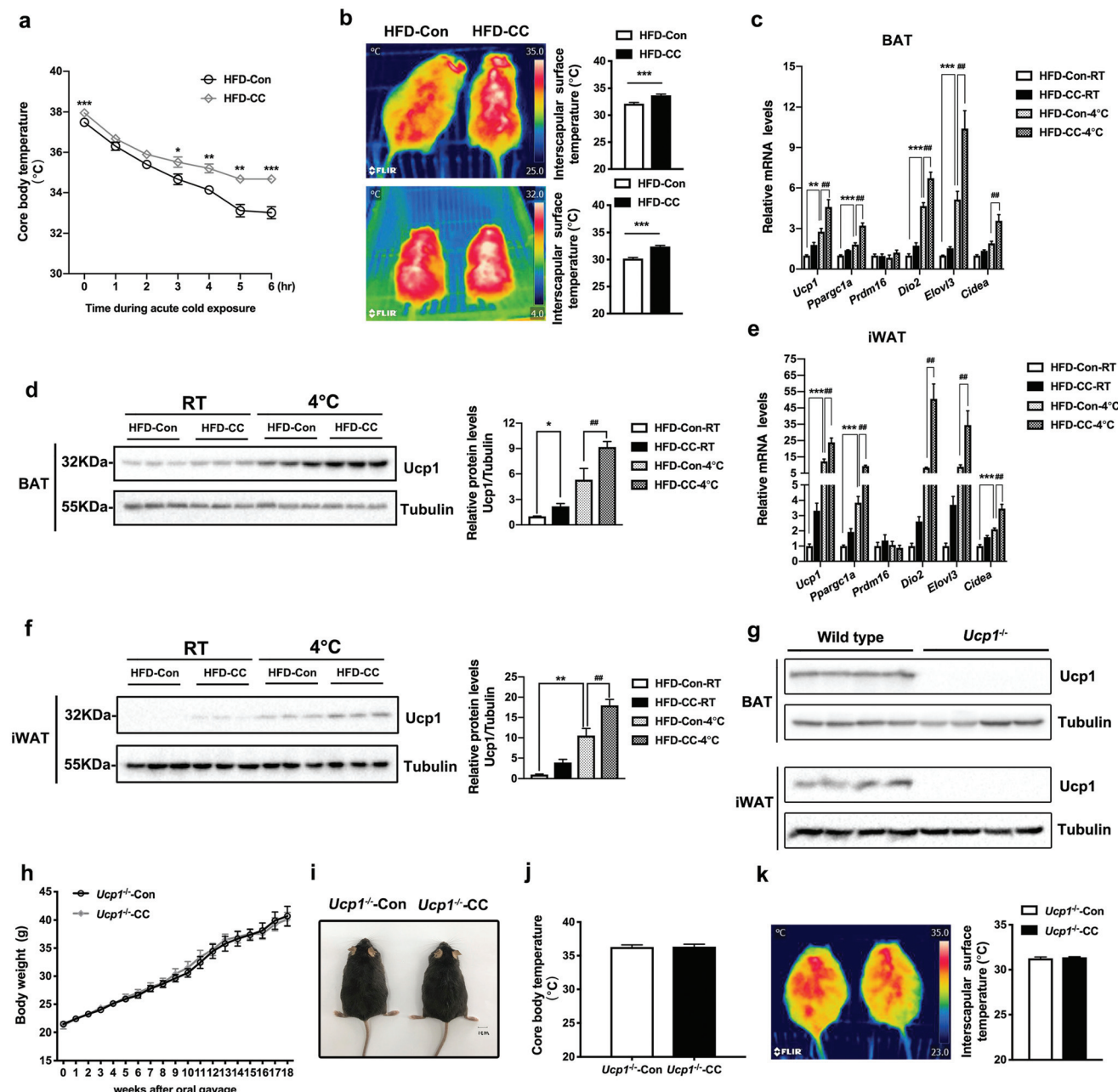


**Fig. 2** Oral administration of curcumin enhances cold tolerance in HFD-fed mice in a *Ucp1*-dependent manner. (a) The rectal temperature of HFD-fed mice treated with curcumin or vehicle for 8 weeks during acute exposure to cold ( $n = 8$  per group). (b) Representative thermal images (left panel) and dorsal interscapular surface temperature (right panel) of mice in (a) (upper panel, at room temperature; lower panel, at 4 °C for 6 h) ( $n = 8$  per group). (c) Expression of thermogenic genes in BAT from HFD-fed mice treated with curcumin or vehicle for 8 weeks after acute exposure to cold for 6 h ( $n = 6$  per group). (d) Western blotting (left panel) and densitometric analyses (right panel) of *Ucp1* in BAT from mice in (c). (e) Expression of thermogenic genes in iWAT from mice in (c) ( $n = 6$  per group). (f) Western blotting (left panel) and densitometric analyses (right panel) of *Ucp1* in iWAT from mice in (c). (g) Western blotting of *Ucp1* in BAT and iWAT from wild type and *Ucp1*<sup>-/-</sup> mice. (h) Bodyweight gain of curcumin- and vehicle-treated *Ucp1*<sup>-/-</sup> mice during HFD feeding ( $n = 7$  or 8 per group). (i) A representative photograph of HFD-fed *Ucp1*<sup>-/-</sup> mice treated with curcumin or vehicle for 18 weeks. (j) Rectal temperature of HFD-fed *Ucp1*<sup>-/-</sup> mice treated with curcumin or vehicle for 8 weeks at room temperature ( $n = 8$  per group). (k) Thermal images (left panel), and dorsal interscapular surface temperatures (right panel) of HFD-fed *Ucp1*<sup>-/-</sup> mice treated with curcumin or vehicle for 18 weeks at room temperature. For results in (c–f),  $^{##}P < 0.01$  for curcumin-treated HFD-fed mice after acute exposure to cold versus vehicle-treated HFD-fed mice after acute exposure to cold. Numerical data are shown as the mean  $\pm$  SEM. \* $P < 0.05$ , \*\* $P < 0.01$ , \*\*\* $P < 0.001$ .

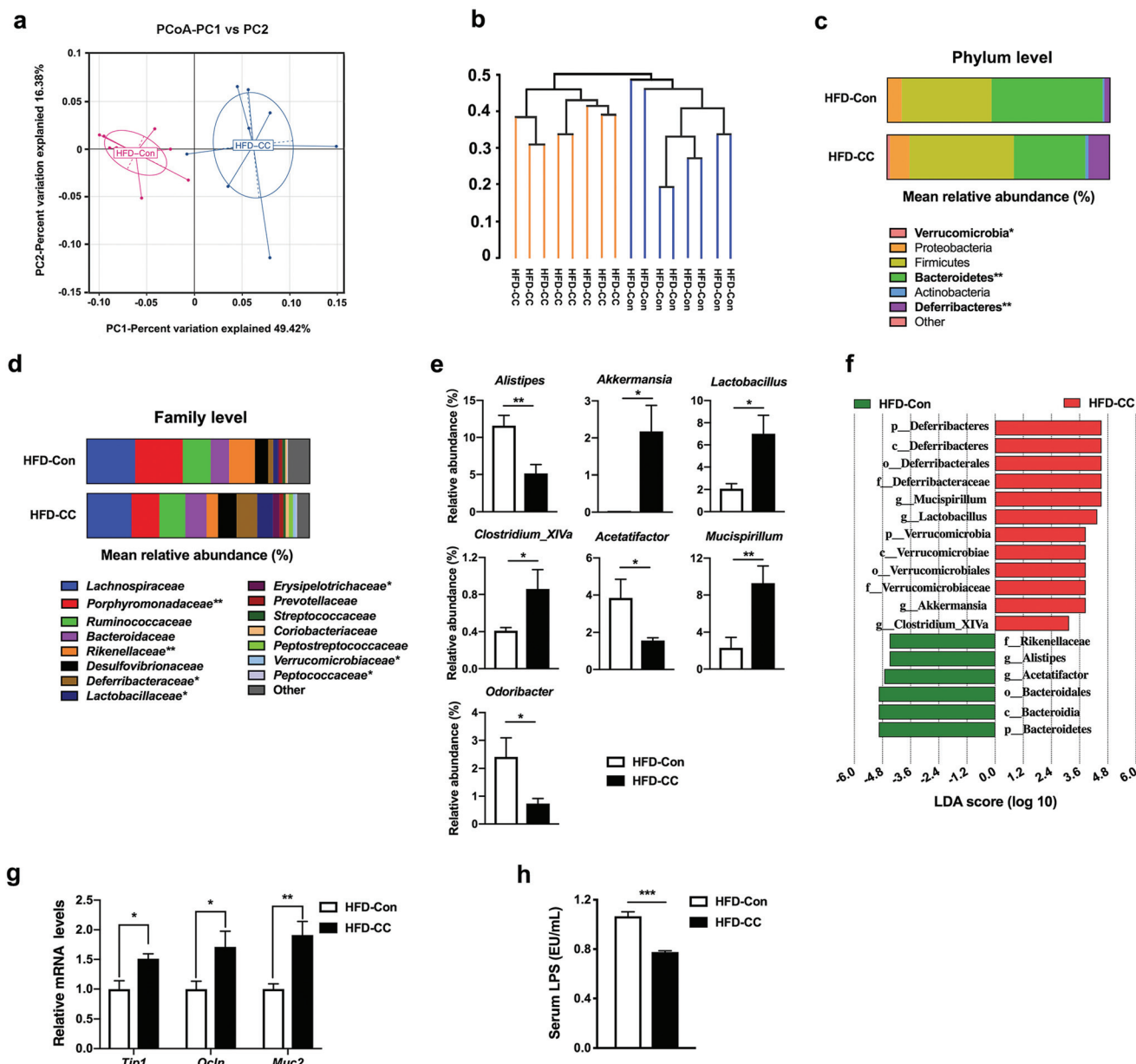


**Fig. 3** Oral administration of curcumin alters the GM in HFD-fed mice. (a) Weighted Unifrac distance-based PCoA analysis of the GM in HFD-fed mice treated with curcumin or vehicle for 3 weeks ( $n = 8$  per group). (b) Hierarchical clustering tree of the GM from mice in (a) using the UPGMA algorithm. (c, d) Average relative abundance of gut bacteria at phylum (c) and family (d) levels from mice in (a). (e) Relative abundance of significantly altered gut bacteria at the genus level from mice in (a). (f) Discriminative taxa determined by LEfSe of the GM from mice in (a) ( $\log_{10}$  LDA  $> 2.0$ ). (g) Expression of mucosal defense genes in the ileum from HFD-fed mice treated with curcumin or vehicle for 3 weeks ( $n = 6$  per group). (h) Plasma levels of LPS in HFD-fed mice treated with curcumin or vehicle for 12 weeks ( $n = 8$  per group). Numerical data are shown as the mean  $\pm$  SEM. \* $P < 0.05$ , \*\* $P < 0.01$ , \*\*\* $P < 0.001$ .

results indicated that oral treatment with curcumin shaped the GM community and ameliorated HFD-induced GM dysbiosis.

#### Gut microbiota mediates the enhanced effects of curcumin on Ucp1-dependent thermogenesis

FMT experiments were undertaken to ascertain if the GM orchestrated the curcumin-induced attenuation of HFD-

induced obesity. Quantitative real-time PCR of the fecal microbiota obtained from recipient mice implied that FMT caused a similar change in GM composition at phylum and genus levels when compared with the change between donor mice (ESI Fig. 4†). Transplantation of curcumin-restructured fecal microbiota mimicked the effects of curcumin on ameliorating HFD-induced obesity (Fig. 4a–c and ESI Fig. 5†). Moreover, endogenous GM-depleted mice colonized with the microbiota

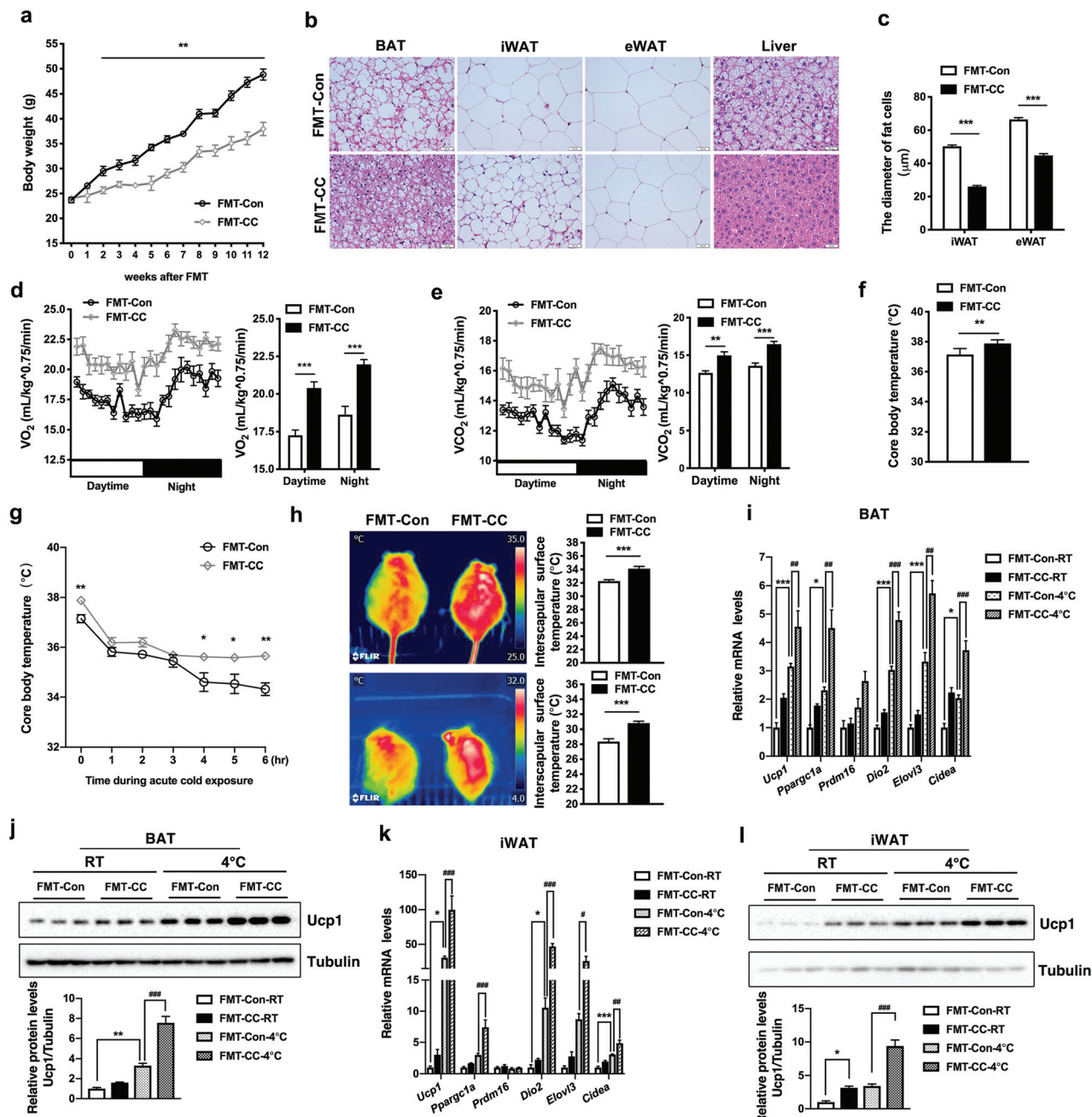


**Fig. 4** The enhanced effect of curcumin on Ucp1-dependent thermogenesis is dependent on the GM. (a) Bodyweight gain of endogenous GM-depleted mice colonized with the microbiota harvested from curcumin- and vehicle-treated HFD-fed mice during HFD feeding ( $n = 8$  per group). (b, c) Representative H&E staining (b) of BAT, iWAT, eWAT and liver and average diameters of fat cells (c) from endogenous GM-depleted HFD-fed mice colonized with the microbiota harvested from HFD-fed mice treated with curcumin or vehicle for 12 weeks. Scale bar,  $20 \mu\text{m}$ . (d) Rate of  $O_2$  consumption (left panel) and average rate of  $O_2$  consumption (right panel) of bodyweight-matched endogenous GM-depleted HFD-fed mice after colonization with the microbiota harvested from HFD-fed mice treated with curcumin or vehicle for 3 weeks ( $n = 8$  per group). (e) Rate of  $CO_2$  production (left panel) and average rate of  $CO_2$  production (right panel) of mice in (d) ( $n = 8$  per group). (f) Rectal temperature of endogenous GM-depleted HFD-fed mice after colonization with the microbiota harvested from HFD-fed mice treated with curcumin or vehicle for 8 weeks at room temperature ( $n = 6$  per group). (g) Rectal temperature of mice in (f) during acute exposure to cold ( $n = 6$  per group). (h) Representative thermal images (left panel) and dorsal interscapular surface temperature (right panel) of mice in (f) during acute exposure to cold (upper panel, at room temperature; lower panel, at  $4^{\circ}\text{C}$  for 6 h). (i) Expression of thermogenic genes in BAT from mice in (f) after acute exposure to cold for 6 h ( $n = 6$  per group). (j) Western blotting (upper panel) and densitometric analyses (lower panel) of Ucp1 in BAT from mice in (i). (k) Expression of thermogenic genes in iWAT from mice in (f) after acute exposure to cold for 6 h ( $n = 6$  per group). (l) Western blotting (upper panel) and densitometric analyses (lower panel) of Ucp1 in iWAT from mice in (k). For results in (i–l),  $^{\#}P < 0.05$ ,  $^{\#\#}P < 0.01$ ,  $^{\#\#\#}P < 0.001$  endogenous GM-depleted HFD-fed mice colonized with the microbiota harvested from curcumin-treated HFD-fed mice after acute exposure to cold versus endogenous GM-depleted HFD-fed mice colonized with the microbiota harvested from vehicle-treated HFD-fed mice after acute exposure to cold. Numerical data are shown as the mean  $\pm$  SEM. \* $P < 0.05$ , \*\* $P < 0.01$ , \*\*\* $P < 0.001$ .

from curcumin-treated HFD-fed mice showed increased energy expenditure compared with endogenous GM-depleted mice colonized with the microbiota from vehicle-treated HFD-fed mice (Fig. 4d, e and ESI Fig. 6†). Furthermore, an increased core body temperature was observed in mice colonized with the microbiota from curcumin-treated HFD-fed mice (Fig. 4f). Upon acute exposure to cold, the mice colonized with the microbiota from curcumin-treated HFD-fed mice were more resistant to cold stress due to intensified Ucp1-dependent thermogenesis in BAT and iWAT (Fig. 4g–l). In addition, after the endogenous GM had been depleted, the morphology of fecal pellets from curcumin- and vehicle-treated HFD-fed mice changed significantly (ESI Fig. 7a†). After depletion of endogenous GM, the core body temperature was similar between curcumin- and vehicle-treated HFD-fed mice at room temperature (ESI Fig. 7b†). Consistent with the similar core body temperature at room temperature, upon acute exposure to cold, endogenous GM-depleted mice from the two groups displayed no significant difference in the reduction of core body temperature (ESI Fig. 7c†). Moreover, cold-induced expression of thermogenic genes in BAT and iWAT intensified by oral treatment with curcumin disappeared in endogenous GM-depleted mice (ESI Fig. 7d–g†). These results demonstrated that curcumin was reliant on the GM to enhance Ucp1-dependent thermogenesis.

#### **Curcumin influences BA metabolism through the GM in HFD-fed mice**

16S ribosomal DNA sequencing analysis hinted that oral administration of curcumin may increase the production of DCA and LCA. The circulating BA composition, rather than BA pool size, plays an important role in the regulation of energy metabolism.<sup>34,35</sup> Indeed, curcumin treatment modulated the circulating BA composition, most notably increasing the fractions of primary BA beta-muricholic acid ( $\beta$ -MCA), mainly converted *via* the alternative pathway and several secondary BAs, including DCA and LCA while decreasing the fraction of primary BA tauro-cholic acid (TCA), mainly converted *via* the classical pathway (Fig. 5a). Given that the GM has a strong regulatory role in hepatic BA synthesis, the expression of key enzymes involved in hepatic BA synthesis was measured.<sup>14</sup> Hepatic expression of Cyp7a1 and Cyp8b1 which are key enzymes involved in the classical pathway was reduced in curcumin-treated HFD-fed mice, whereas the expression of Cyp7b1 which is a key enzyme involved in the alternative pathway was induced by curcumin (Fig. 5b and c). Interestingly, the expression of these enzymes became comparable between the two groups after GM depletion, implying that GM is involved in the regulatory effects of curcumin on hepatic BA synthesis (Fig. 5d). In contrast, transplantation of the fecal microbiota from curcumin-treated HFD-fed mice influenced hepatic BA synthesis in recipient mice through inducing the expression of Cyp7b1 but reducing that of Cyp7a1 and Cyp8b1, similar to that in their donors (Fig. 5e). Importantly, recipient mice colonized with the microbiota from curcumin-treated HFD-fed mice also showed decreased fractions of circulating

TCA, and increased fractions of circulating DCA and LCA, compared with those in mice colonized with the microbiota from vehicle-treated HFD-fed mice, similar to their donors (Fig. 5f). Taken together, these data suggested that curcumin-restructured GM promoted an alternative pathway of BA synthesis with “sacrifice” of the classical pathway of BA synthesis, and influenced the circulating BA composition.

#### **Curcumin requires TGR5 to enhance Ucp1-dependent thermogenesis**

Expression of the most potent ligands for TGR5 (*i.e.*, LCA and DCA) was in the circulation by oral curcumin treatment and curcumin-restructured FMT. Hence, HFD-fed *Gpbar1*<sup>-/-</sup> mice were used to ascertain if the enhanced effects of curcumin on Ucp1-dependent thermogenesis were reliant on TGR5. TGR5 expression was not detected in the BAT or iWAT of *Gpbar1*<sup>-/-</sup> mice (Fig. 6a). Oral treatment with curcumin increased the fractions of circulating DCA and LCA in HFD-fed *Gpbar1*<sup>-/-</sup> mice (Fig. 6b). However, TGR5 knockout eliminated the effects of curcumin on attenuating HFD-induced obesity (Fig. 6c). Moreover, the core body temperature of HFD-fed *Gpbar1*<sup>-/-</sup> mice was similar between the two groups (Fig. 6d). Upon acute exposure to cold, HFD-fed *Gpbar1*<sup>-/-</sup> mice from the two groups displayed no difference in the reduction of core body temperature and cold-induced expression of thermogenic genes in BAT and iWAT (Fig. 6e–j). These results demonstrated the dependence of curcumin on TGR5 to enhance Ucp1-dependent thermogenesis and ameliorate HFD-induced obesity.

#### **Curcumin stimulates cAMP/PKA signaling in thermogenic adipose tissue through GM and TGR5**

TGR5 undertakes critical functions in energy metabolism by increasing cAMP production, which activates cAMP/PKA signaling pathway to enhance Ucp1-dependent thermogenesis in BAT and iWAT.<sup>19,36</sup> We needed to ascertain if cAMP/PKA signaling pathway could be activated in thermogenic adipose tissue by curcumin. Curcumin treatment and curcumin-restructured FMT increased intracellular cAMP levels in BAT and iWAT (Fig. 7a and b). As expected, phosphorylation of Creb which is the downstream of the cAMP/PKA signaling pathway was upregulated by curcumin treatment and curcumin-restructured FMT (Fig. 7c and d). Consistent with the appearance of beige adipocytes upon H&E staining of iWAT, the expression of beige-specific marker genes was induced in iWAT by curcumin treatment and curcumin-restructured FMT (Fig. 7e and f). Transmission electron microscopy suggested an increased number of mitochondria in thermogenic adipose tissue from curcumin-treated HFD-fed mice (Fig. 7g). Consistently, the expression of key transcription factors involved in mitochondrial biogenesis and mitochondrial number were increased in BAT and iWAT from curcumin-treated HFD-fed mice and their recipients (Fig. 7h and i). However, activation of the cAMP/PKA signaling pathway by curcumin in BAT and iWAT was abolished by TGR5 knockout (Fig. 8a and b). Moreover, the expression of beige-specific marker genes was comparable between curcumin- and vehicle-treated HFD-fed *Gpbar1*<sup>-/-</sup>

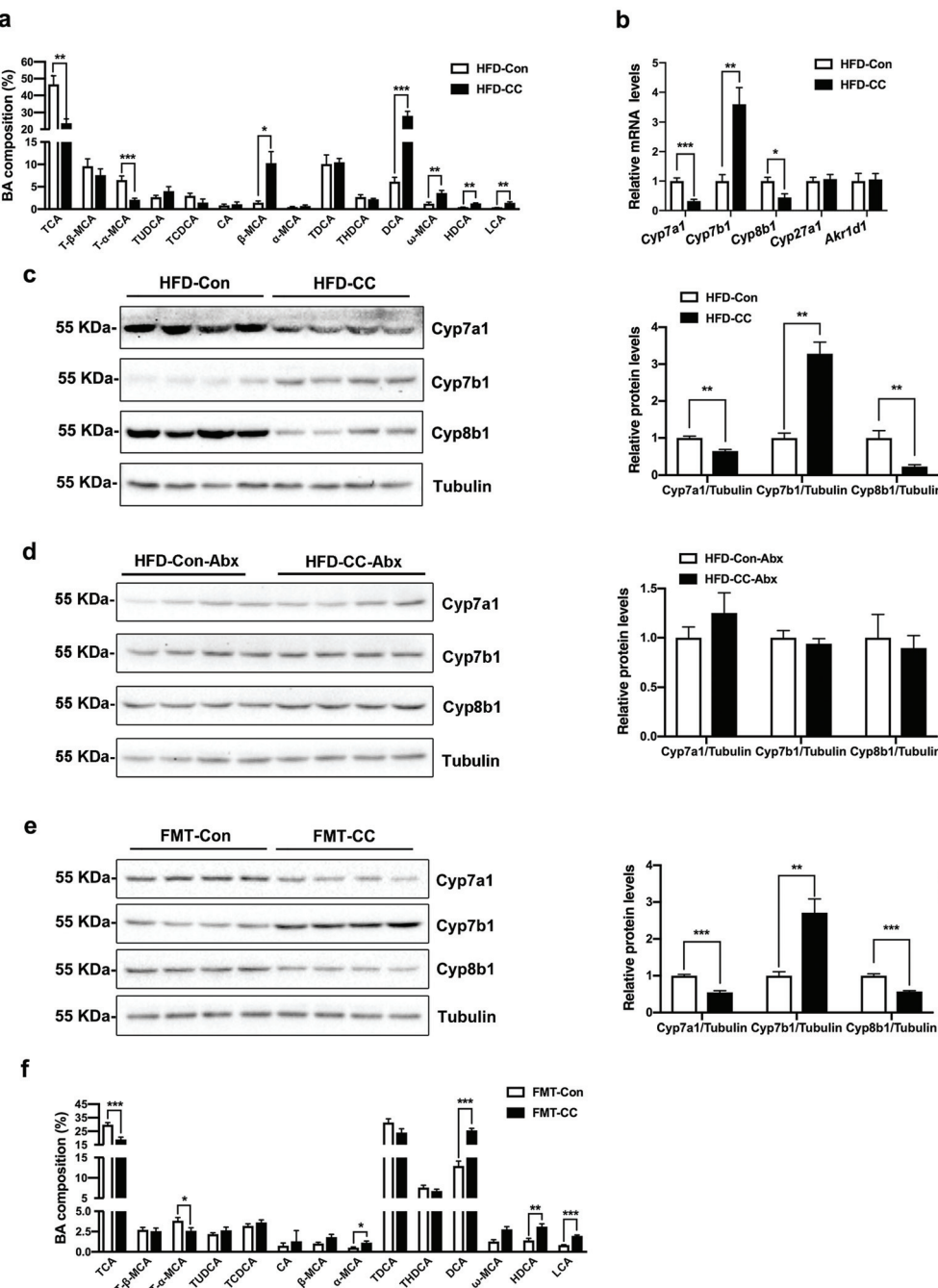


**Fig. 5** GM mediates the effects of curcumin on BA metabolism in HFD-fed mice. (a) Serum BA composition of HFD-fed mice treated with curcumin or vehicle for 3 weeks ( $n = 8$  per group). (b) Expression of genes involved in BA metabolism in mice treated as in (a) ( $n = 6$  per group). (c) Western blotting (left panel) and densitometric analyses (right panel) of Cyp7a1, Cyp7b1 and Cyp8b1 in the liver from mice in (a). (d) Western blotting (left panel) and densitometric analyses (right panel) of Cyp7a1, Cyp7b1 and Cyp8b1 in the liver from curcumin- and vehicle-treated HFD-fed mice after antibiotic treatment for 4 weeks. (e) Western blotting (upper panel) and densitometric analyses (lower panel) of Cyp7a1, Cyp7b1 and Cyp8b1 in the liver from endogenous GM-depleted HFD-fed mice after colonization with the microbiota harvested from HFD-fed mice treated with curcumin or vehicle for 3 weeks. (f) Serum BA composition of mice treated as in (e) ( $n = 8$  per group). Numerical data are shown as the mean  $\pm$  SEM. \* $P < 0.05$ , \*\* $P < 0.01$ , \*\*\* $P < 0.001$ .

mice (Fig. 8c). Furthermore, curcumin-induced mitochondrial biogenesis in BAT and iWAT was eliminated in *Gpbar1*<sup>-/-</sup> mice (Fig. 8d). Most importantly, the data suggested that the GM

and TGR5 mediated the effects of curcumin by upregulating the cAMP/PKA signaling pathway in thermogenic adipose tissue.

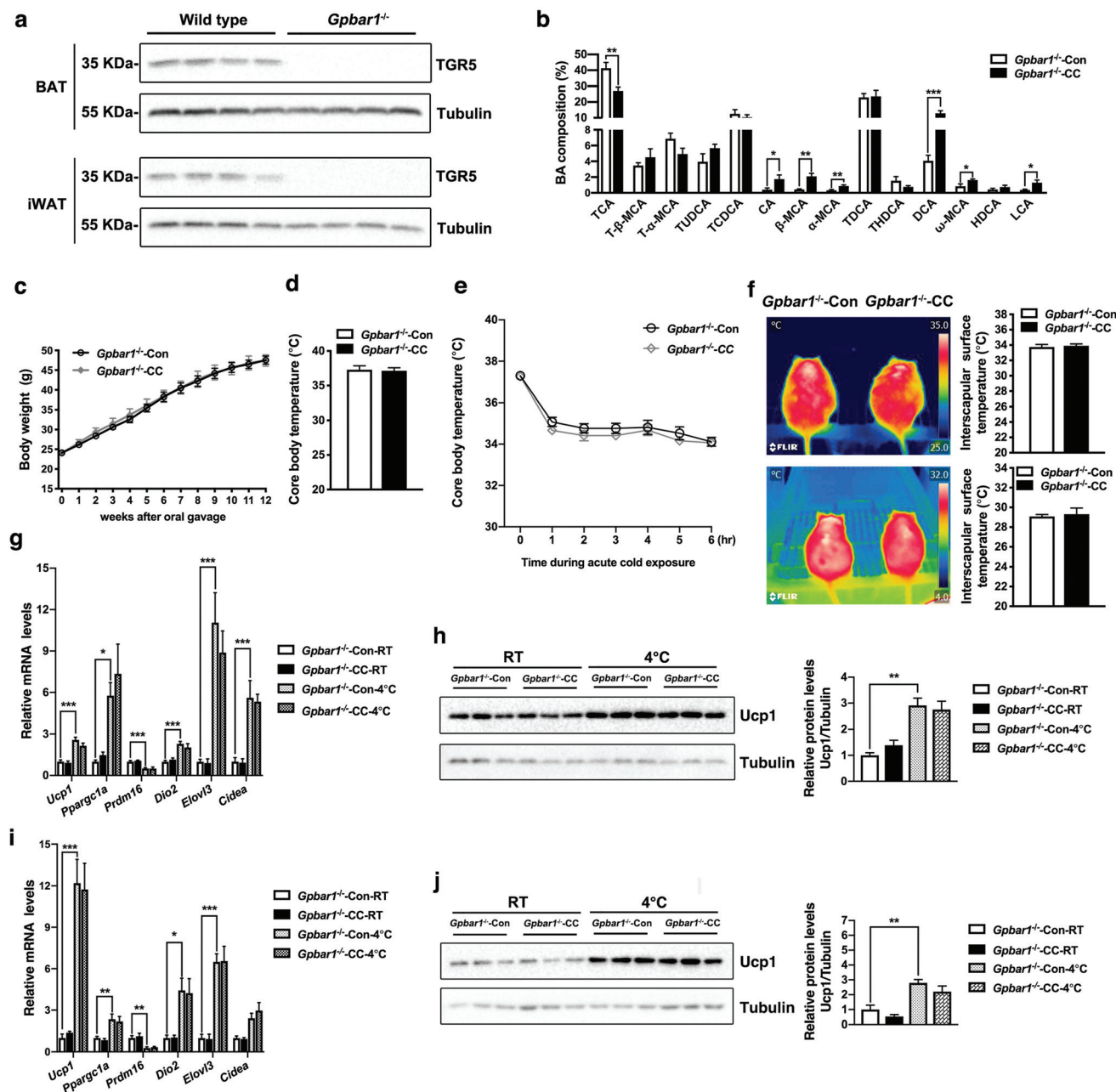


**Fig. 6** Curcumin requires TGR5 to enhance Ucp1-dependent thermogenesis. (a) Western blotting of TGR5 in BAT and iWAT from wild type and *Gpbar1<sup>-/-</sup>* mice. (b) Serum BA composition of HFD-fed *Gpbar1<sup>-/-</sup>* mice treated with curcumin or vehicle for 3 weeks ( $n = 8$  per group). (c) Body weight gain of curcumin- and vehicle-treated *Gpbar1<sup>-/-</sup>* mice during HFD feeding ( $n = 10$  per group). (d) Rectal temperature of curcumin- and vehicle-treated *Gpbar1<sup>-/-</sup>* mice at room temperature during HFD feeding ( $n = 8$  per group). (e) Rectal temperature of mice in (c) during acute exposure to cold ( $n = 8$  per group). (f) Representative thermal images (left panel) and dorsal interscapular surface temperature (right panel) of mice in (c) during acute exposure to cold (upper panel, at room temperature; lower panel, at 4 °C for 6 h). (g) Expression of thermogenic genes in BAT from HFD-fed *Gpbar1<sup>-/-</sup>* mice treated with curcumin or vehicle for 8 weeks after acute exposure to cold for 6 h ( $n = 6$  per group). (h) Western blotting (left panel) and densitometric analyses (right panel) of Ucp1 in BAT from mice in (f). (i) Expression of thermogenic genes in iWAT from HFD-fed *Gpbar1<sup>-/-</sup>* mice treated with curcumin or vehicle for 8 weeks after acute exposure to cold for 6 h ( $n = 6$  per group). (j) Western blotting (left panel) and densitometric analyses (right panel) of Ucp1 in iWAT from mice in (i). Numerical data are shown as the mean  $\pm$  SEM. \* $P < 0.05$ , \*\* $P < 0.01$ , \*\*\* $P < 0.001$ .

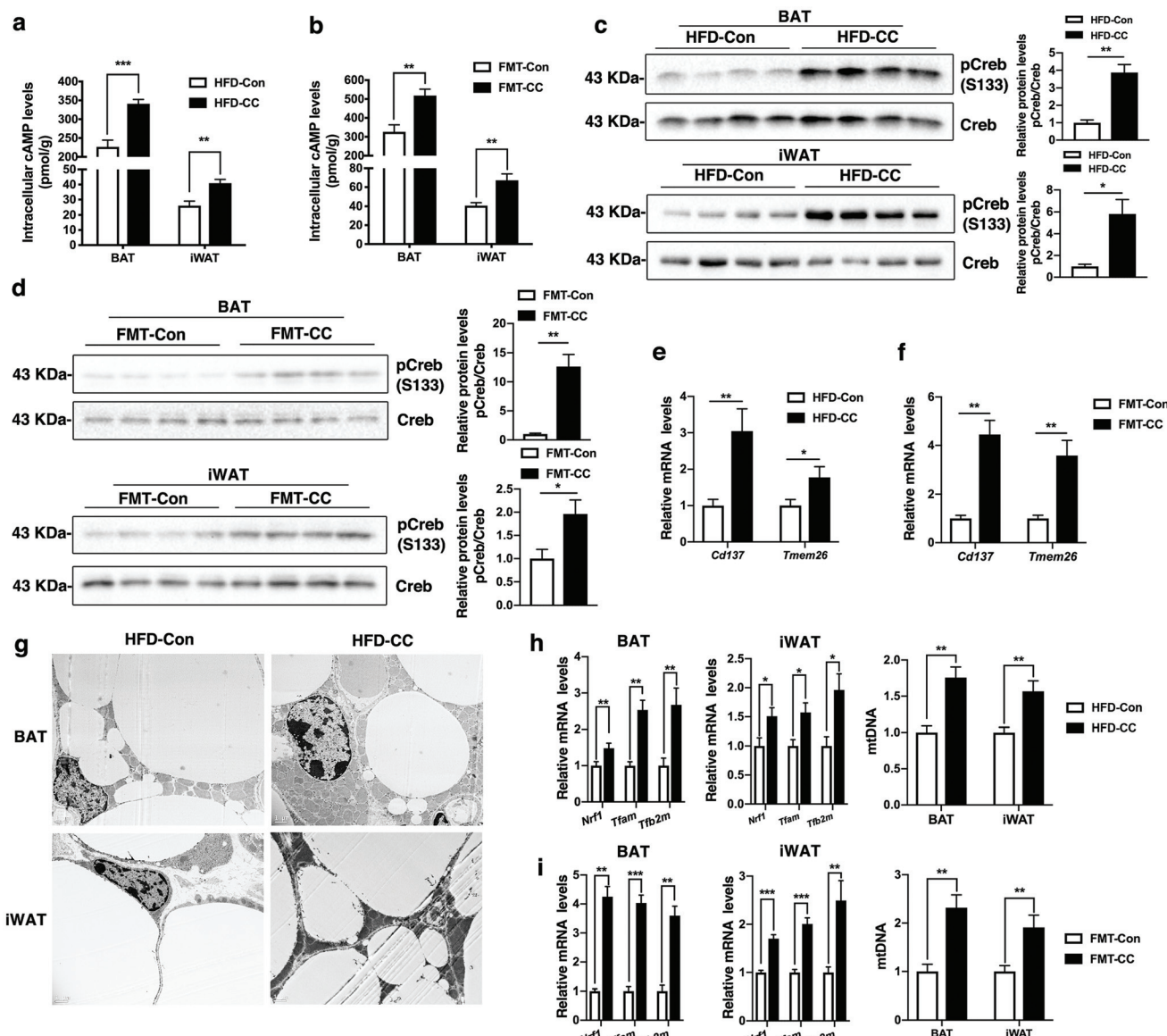


**Fig. 7** Curcumin upregulates the cAMP/PKA signaling pathway in thermogenic adipose tissue through the GM. (a, b) cAMP levels in BAT and iWAT from HFD-fed mice treated with curcumin or vehicle (a) and endogenous GM-depleted HFD-fed mice colonized with the microbiota harvested from curcumin- and vehicle-treated HFD-fed mice (b) for 3 weeks ( $n = 6$  per group). (c, d) Western blotting (left panel) and densitometric analyses (right panel) of phosphorylated Creb and total Creb in BAT (upper panel) and iWAT (lower panel) extracts from HFD-fed mice treated with curcumin or vehicle (c) and endogenous GM-depleted HFD-fed mice colonized with the microbiota harvested from curcumin- and vehicle-treated HFD-fed mice (d) for 3 weeks. (e, f) Expression of beige cell marker genes in iWAT from HFD-fed mice treated with curcumin or vehicle (e) and endogenous GM-depleted HFD-fed mice colonized with the microbiota harvested from curcumin- and vehicle-treated HFD-fed mice (f) for 8 weeks ( $n = 6$  per group). (g) Transmission electron microscopy of BAT and iWAT from HFD-fed mice treated with curcumin or vehicle for 8 weeks. Scale bar, 1  $\mu\text{m}$ . (h, i) Expression of genes involved in mitochondrial biogenesis in BAT (left panel) and iWAT (middle panel) and relative mtDNA content (right panel) in BAT and iWAT from HFD-fed mice treated with curcumin or vehicle (h) and endogenous GM-depleted HFD-fed mice colonized with the microbiota harvested from curcumin- and vehicle-treated HFD-fed mice (i) for 8 weeks ( $n = 6$  per group). Numerical data are shown as the mean  $\pm$  SEM. \* $P < 0.05$ , \*\* $P < 0.01$ , \*\*\* $P < 0.001$ .

## Discussion

Phytochemicals have garnered interest in preventing and treating metabolic diseases.<sup>37</sup> However, phytochemicals have poor bioavailability, so the possibility of phytochemicals producing beneficial effects and the mechanisms by which phytochem-

icals carry out their physiological functions are still controversial.<sup>38</sup> Increasingly, it is being appreciated that the GM is a metabolic “organ” that influences the host metabolism by producing numerous metabolites which act as ligands to activate specific signaling pathways. Thus, it is necessary to explore the connection between phytochemicals and the GM.<sup>16,39</sup>

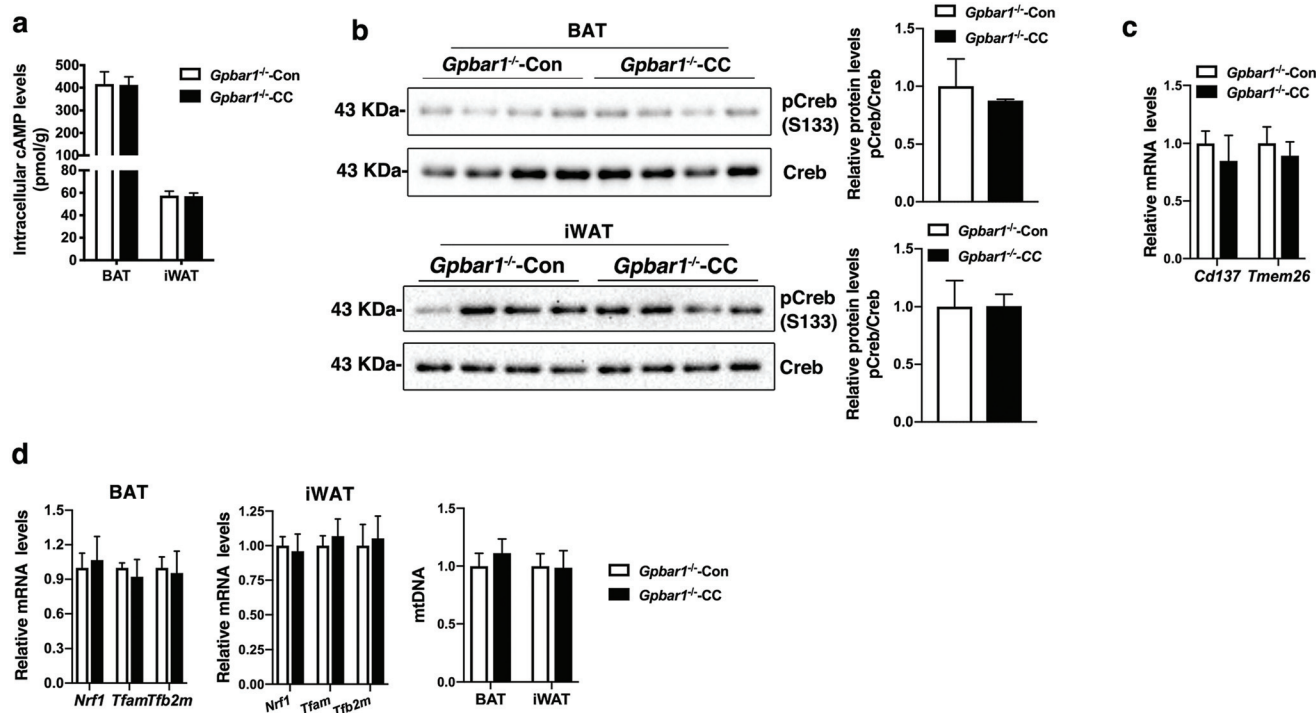


**Fig. 8** Curcumin needs TGR5 to activate the cAMP/PKA signaling pathway in thermogenic adipose tissue. (a) cAMP levels in BAT and iWAT from HFD-fed *Gpbar<sup>1-/-</sup>* mice treated with curcumin or vehicle for 3 weeks ( $n = 6$  per group). (b) Western blotting (left panel) and densitometric analyses (right panel) of phosphorylated Creb and total Creb in BAT (upper panel) and iWAT (lower panel) extracts from HFD-fed mice treated with curcumin or vehicle for 3 weeks. (c) Expression of beige cell marker genes in iWAT from HFD-fed *Gpbar<sup>1-/-</sup>* mice treated with curcumin or vehicle for 8 weeks ( $n = 6$  per group). (d) Expression of genes involved in mitochondrial biogenesis in BAT (left panel) and iWAT (middle panel) and relative mtDNA content (right panel) in BAT and iWAT from HFD-fed *Gpbar<sup>1-/-</sup>* mice treated with curcumin or vehicle for 8 weeks ( $n = 6$  per group). Numerical data are shown as the mean  $\pm$  SEM.

Although curcumin has multiple beneficial effects on improving metabolic dysfunction, the precise mechanism underpinning the ability of curcumin to alleviate obesity is not known. Recently, curcumin has been reported to promote the activity of BAT and browning of iWAT. However, the mechanism underlying its enhancement of adaptive thermogenesis and the contribution of Ucp1-dependent thermogenesis to the anti-obesity effects of curcumin are not known.<sup>8,9</sup> Therefore, we used HFD-fed *Ucp1<sup>1-/-</sup>* mice to reveal the dependence of curcumin on Ucp1-dependent thermogenesis to ameliorate HFD-induced obesity. Although curcumin has been demonstrated to increase intracellular level of cAMP, the underlying mechanism has not been elucidated.<sup>40</sup> HFD-fed *Gpbar<sup>1-/-</sup>* mice were used to validate the hypothesis that curcumin can increase cAMP production through TGR5. TGR5 knockout was found to eliminate the enhanced effects of curcumin on Ucp1-dependent thermogenesis, indicating that curcumin enhanced Ucp1-dependent thermogenesis through TGR5.

Data disclosing that curcumin protects against metabolic disorders by improving BA homeostasis and the GM hinted that the gut-to-liver axis is indispensable for the metabolic-improvement effects of curcumin.<sup>41,42</sup> Consistent with those studies, our results indicated that curcumin modulated the GM community and increased the relative abundance of

*Lactobacillus* and *Clostridium* cluster XIVa involved in the microbial modifications of BA. The GM not only regulates the metabolism of secondary BAs, it also influences hepatic BA synthesis.<sup>17</sup> Therefore, the expression of key enzymes involved in BA synthesis was measured, and our results suggested that curcumin inhibited the classical pathway for BA synthesis but induced the alternative pathway for BA synthesis. Increasing numbers of studies have indicated hepatic BA synthesis, characterized by inhibition of the classical pathway and induction of the alternative pathway, to be positively related to the improvement of metabolic dysfunctions by influencing the circulating BA composition.<sup>16,34,43,44</sup> The latter, characterized by an increased fraction of circulating LCA or DCA, resulted from changes in the contribution of hepatic BA synthesis by classical and alternative routes to total BA synthesis. Also, regulation of the GM could activate TGR5 in BAT and iWAT, thereby enhancing Ucp1-dependent thermogenesis through upregulation of the cAMP/PKA signaling pathway.<sup>34,45,46</sup> Ucp1-dependent thermogenesis can dissipate energy to generate heat, so it is a good way to increase energy expenditure and combat obesity. Oral treatment with curcumin and curcumin-restructured FMT both led to reduced fraction of circulating TCA synthesized mainly through a classical pathway of BA synthesis and an increased fraction of circulating LCA which is a second-

ary BA converted from alternative pathway-derived primary BAs. Surprisingly, the fraction of circulating DCA converted from CA was increased by oral treatment with curcumin and curcumin-restructured FMT. This paradoxical result may have been due to three main reasons. First, the classical pathway for BA synthesis contributes to approximately 75% of total BA synthesis in mice.<sup>47</sup> Although curcumin inhibited the expression of Cyp7a1 and Cyp8b1, the contribution of the classical pathway to total BA synthesis cannot be neglected. Second, 16S ribosomal DNA sequencing analysis indicated an increase in the number of *Clostridium* cluster XIVa due to oral treatment with curcumin. The *Clostridium* genus possesses BSH activity, so *Clostridium* cluster XIVa promotes the metabolic conversion of CA to DCA.<sup>32</sup> Third, the BA composition in serum is the combined result of several metabolic pathways, including hepatic BAs synthesis, enterohepatic circulation, microbial modifications, and fecal excretion, which demonstrates that it is not appropriate to make the circulating BA composition represent hepatic BA synthesis. Therefore, although the alternative pathway is induced at the expense of the classical pathway, the fraction of circulating DCA may be increased.

Experiments using FMT and depletion of endogenous GM were conducted to explore the contribution of curcumin-restructured GM on the beneficial effects of curcumin on energy homeostasis. HFD-fed endogenous GM-depleted mice colonized with the microbiota from curcumin-treated HFD-fed mice displayed increased energy expenditure and Ucp1-dependent thermogenesis that was comparable with the characteristics of curcumin-treated HFD-fed mice. Moreover, the beneficial effects of curcumin on Ucp1-dependent thermogenesis were abolished by depletion of endogenous GM. Our results demonstrated the predominant contribution of curcumin-restructured GM to the enhanced effects of curcumin on Ucp1-dependent thermogenesis in HFD-fed mice.

Curcumin increased the relative abundance of *Akkermansia* which is a probiotic that has positive effects on the amelioration of HFD-induced obesity and associated metabolic disorders. In contrast, curcumin decreased the relative abundance of *Alistipes* whose functions are contrary to those of *Akkermansia*.<sup>48</sup> Also, curcumin upregulated the expression of genes involved in mucosal defense and decreased the circulating LPS level. Thus, our data suggested that curcumin not only regulated the circulating BA composition, but also improved HFD-induced GM dysbiosis.

As a probiotic, *Akkermansia* ameliorates HFD-induced obesity and associated metabolic disorders. Moreover, several studies have reported the positive correlations between the relative abundance of *Akkermansia* and energy expenditure.<sup>49,50</sup> However, the mechanisms by which *Akkermansia* regulates energy metabolism remain unclear. The relative abundance of *Akkermansia* has been suggested to be positively associated with the fractions of circulating DCA and LCA.<sup>45,51</sup> In the current study, an increased relative abundance of *Akkermansia* was found in curcumin-treated HFD-fed mice, implying that

*Akkermansia* may be involved in regulating BA metabolism to enhance Ucp1-dependent thermogenesis.

The physiological function of BA is to aid the digestion and absorption of lipids and fat-soluble vitamins. Hence, it is rational that BA metabolism is closely related to the type of diet. We found that curcumin had no effect on the bodyweight of C57BL/6J mice during feeding of a chow diet. This is not the first study to discover that BA metabolism depends on the type of diet to influence energy metabolism.<sup>19,34</sup> Thus, the complex role of BA metabolism in energy homeostasis should be elucidated further.

## Conclusions

We uncovered a novel mechanism whereby curcumin alleviated HFD-induced obesity in mice. The GM mediated the enhanced effect of curcumin on Ucp1-dependent thermogenesis. Curcumin-restructured GM modulated BA metabolism, which led to increased fractions of circulating DCA and LCA. Moreover, curcumin upregulated the cAMP/PKA signaling pathway through the GM and TGR5 to enhance Ucp1-dependent thermogenesis. In our knowledge, this is the first report of the GM being a significant contributor in the increased energy expenditure induced by curcumin. Thus, nutritional and pharmacologic approaches to GM modulation may be important for preventing and treating obesity.

## Author contributions

LY and JHC contributed to the conceptual design of the study. ZQH, LY, and YZ conducted most of the experiments. ZQH analyzed and interpreted the data. YZ assisted with data analyses and interpretation. LY wrote the manuscript. YX, JG, ZZZ, SJF, ZZZ, and SGG contributed to raising mice and genotyping. XNC and SC revised the manuscript. All authors reviewed the results and approved the final version of the manuscript.

## Conflicts of interest

The authors declare no competing interests.

## Acknowledgements

This study was supported by the National Natural Science Foundation of China (81803221), Jilin Education Department Thirteen Five-Year Plan Science and Technology Project (JJKH20191067KJ), Jilin Science and Technology Bureau Innovative Development Project (201831717), and University Innovative Start-up Training Project (202013706032). We thank Lai-Fu Du (Genesky Biotechnology, Shanghai, China) for excellent technical support on 16S ribosomal DNA sequencing analyses.

## References

- 1 P. Gonzalez-Muniesa, M. A. Martinez-Gonzalez, F. B. Hu, J. P. Despres, Y. Matsuzawa, R. J. F. Loos, L. A. Moreno, G. A. Bray and J. A. Martinez, Obesity, *Nat. Rev. Dis. Primers*, 2017, **3**, 17034.
- 2 N. Nagata, L. Xu, S. Kohno, Y. Ushida, Y. Aoki, R. Umeda, N. Fukue, F. Zhuge, Y. Ni, M. Nagashimada, C. Takahashi, H. Suganuma, S. Kaneko and T. Ota, Glucoraphanin Ameliorates Obesity and Insulin Resistance Through Adipose Tissue Browning and Reduction of Metabolic Endotoxemia in Mice, *Diabetes*, 2017, **66**, 1222–1236.
- 3 K. Ikeda, Q. Kang, T. Yoneshiro, J. P. Camporez, H. Maki, M. Homma, K. Shinoda, Y. Chen, X. Lu, P. Maretich, K. Tajima, K. M. Ajuwon, T. Soga and S. Kajimura, UCP1-independent signaling involving SERCA2b-mediated calcium cycling regulates beige fat thermogenesis and systemic glucose homeostasis, *Nat. Med.*, 2017, **23**, 1454–1465.
- 4 S. H. Chang, N. J. Song, J. H. Choi, U. J. Yun and K. W. Park, Mechanisms underlying UCP1 dependent and independent adipocyte thermogenesis, *Obes. Rev.*, 2019, **20**, 241–251.
- 5 A. M. Cypress, S. Lehman, G. Williams, I. Tal, D. Rodman, A. B. Goldfine, F. C. Kuo, E. L. Palmer, Y. H. Tseng, A. Doria, G. M. Kolodny and C. R. Kahn, Identification and importance of brown adipose tissue in adult humans, *N. Engl. J. Med.*, 2009, **360**, 1509–1517.
- 6 K. A. Virtanen, M. E. Lidell, J. Orava, M. Heglin, R. Westergren, T. Niemi, M. Taittonen, J. Laine, N. J. Savisto, S. Enerback and P. Nuutila, Functional brown adipose tissue in healthy adults, *N. Engl. J. Med.*, 2009, **360**, 1518–1525.
- 7 S. Shishodia, Molecular mechanisms of curcumin action: gene expression, *BioFactors*, 2013, **39**, 37–55.
- 8 Z. Song, X. Revelo, W. Shao, L. Tian, K. Zeng, H. Lei, H.-S. Sun, M. Woo, D. Winer and T. Jin, Dietary Curcumin Intervention Targets Mouse White Adipose Tissue Inflammation and Brown Adipose Tissue UCP1 Expression, *Obesity*, 2018, **26**, 547–558.
- 9 S. Wang, X. Wang, Z. Ye, C. Xu, M. Zhang, B. Ruan, M. Wei, Y. Jiang, Y. Zhang, L. Wang, X. Lei and Z. Lu, Curcumin promotes browning of white adipose tissue in a norepinephrine-dependent way, *Biochem. Biophys. Res. Commun.*, 2015, **466**, 247–253.
- 10 L. Shen and H. F. Ji, Bidirectional interactions between dietary curcumin and gut microbiota, *Crit. Rev. Food Sci. Nutr.*, 2019, **59**, 2896–2902.
- 11 A. L. Lopresti, The Problem of Curcumin and Its Bioavailability: Could Its Gastrointestinal Influence Contribute to Its Overall Health-Enhancing Effects?, *Adv. Nutr.*, 2018, **9**, 41–50.
- 12 L. Zhao, The gut microbiota and obesity: from correlation to causality, *Nat. Rev. Microbiol.*, 2013, **11**, 639–647.
- 13 V. K. Ridaura, J. J. Faith, F. E. Rey, J. Cheng, A. E. Duncan, A. L. Kau, N. W. Griffin, V. Lombard, B. Henrissat, J. R. Bain, M. J. Muehlbauer, O. Ilkayeva, C. F. Semenkovich, K. Funai, D. K. Hayashi, B. J. Lyle, M. C. Martini, L. K. Ursell, J. C. Clemente, W. Van Treuren, W. A. Walters, R. Knight, C. B. Newgard, A. C. Heath and J. I. Gordon, Gut microbiota from twins discordant for obesity modulate metabolism in mice, *Science*, 2013, **341**, 1241214.
- 14 A. Wahlstrom, S. I. Sayin, H. U. Marschall and F. Backhed, Intestinal Crosstalk between Bile Acids and Microbiota and Its Impact on Host Metabolism, *Cell Metab.*, 2016, **24**, 41–50.
- 15 A. Di Ciaula, G. Garruti, R. Lunardi Baccetto, E. Molina-Molina, L. Bonfrate, D. Q. H. Wang and P. Portincasa, Bile Acid Physiology, *Ann. Hepatol.*, 2017, **16**, S4–S14.
- 16 F. Huang, X. Zheng, X. Ma, R. Jiang, W. Zhou, S. Zhou, Y. Zhang, S. Lei, S. Wang, J. Kuang, X. Han, M. Wei, Y. You, M. Li, Y. Li, D. Liang, J. Liu, T. Chen, C. Yan, R. Wei, C. Rajani, C. Shen, G. Xie, Z. Bian, H. Li, A. Zhao and W. Jia, Theabrownin from Pu-erh tea attenuates hypercholesterolemia via modulation of gut microbiota and bile acid metabolism, *Nat. Commun.*, 2019, **10**, 4971.
- 17 S. I. Sayin, A. Wahlstrom, J. Felin, S. Jantti, H. U. Marschall, K. Bamberg, B. Angelin, T. Hyotylainen, M. Oresic and F. Backhed, Gut microbiota regulates bile acid metabolism by reducing the levels of tauro-beta-muricholic acid, a naturally occurring FXR antagonist, *Cell Metab.*, 2013, **17**, 225–235.
- 18 E. P. Broeders, E. B. Nascimento, B. Havekes, B. Brans, K. H. Roumans, A. Tailleux, G. Schaat, M. Kouach, J. Charton, B. Deprez, N. D. Bouvy, F. Mottaghy, B. Staels, W. D. van Marken Lichtenbelt and P. Schrauwen, The Bile Acid Chenodeoxycholic Acid Increases Human Brown Adipose Tissue Activity, *Cell Metab.*, 2015, **22**, 418–426.
- 19 M. Watanabe, S. M. Houten, C. Mataki, M. A. Christoffolete, B. W. Kim, H. Sato, N. Messaddeq, J. W. Harney, O. Ezaki, T. Kodama, K. Schoonjans, A. C. Bianco and J. Auwerx, Bile acids induce energy expenditure by promoting intracellular thyroid hormone activation, *Nature*, 2006, **439**, 484–489.
- 20 M. Vijay-Kumar, J. D. Aitken, F. A. Carvalho, T. C. Cullender, S. Mwangi, S. Srinivasan, S. V. Sitaraman, R. Knight, R. E. Ley and A. T. Gewirtz, Metabolic syndrome and altered gut microbiota in mice lacking Toll-like receptor 5, *Science*, 2010, **328**, 228–231.
- 21 F. Li, C. Jiang, K. W. Krausz, Y. Li, I. Albert, H. Hao, K. M. Fabre, J. B. Mitchell, A. D. Patterson and F. J. Gonzalez, Microbiome remodelling leads to inhibition of intestinal farnesoid X receptor signalling and decreased obesity, *Nat. Commun.*, 2013, **4**, 2384.
- 22 Y. W. Yang, M. K. Chen, B. Y. Yang, X. J. Huang, X. R. Zhang, L. Q. He, J. Zhang and Z. C. Hua, Use of 16S rRNA Gene-Targeted Group-Specific Primers for Real-Time PCR Analysis of Predominant Bacteria in Mouse Feces, *Appl. Environ. Microbiol.*, 2015, **81**, 6749–6756.
- 23 H. S. Ejtahed, Z. Hoseini-Tavassoli, S. Khatami, M. Zangeneh, A. Behrouzi, S. Ahmadi Badi, A. Moshiri, S. Hasani-Ranjbar, A. R. Soroush, F. Vaziri, A. Fateh,

- M. Ghanei, S. Bouzari, S. Najar-Peerayeh, S. D. Siadat and B. Larijani, Main gut bacterial composition differs between patients with type 1 and type 2 diabetes and non-diabetic adults, *J. Diabetes Metab. Disord.*, 2020, **19**, 265–271.
- 24 G. Duytschaever, G. Huys, M. Bekaert, L. Boulanger, K. De Boeck and P. Vandamme, Dysbiosis of bifidobacteria and Clostridium cluster XIVa in the cystic fibrosis fecal microbiota, *J. Cystic Fibrosis*, 2013, **12**, 206–215.
- 25 H. Lin, Y. An, H. Tang and Y. Wang, Alterations of Bile Acids and Gut Microbiota in Obesity Induced by High Fat Diet in Rat Model, *J. Agric. Food Chem.*, 2019, **67**, 3624–3632.
- 26 N. L. Price, A. P. Gomes, A. J. Ling, F. V. Duarte, A. Martin-Montalvo, B. J. North, B. Agarwal, L. Ye, G. Ramadori, J. S. Teodoro, B. P. Hubbard, A. T. Varela, J. G. Davis, B. Varamini, A. Hafner, R. Moaddel, A. P. Rolo, R. Coppari, C. M. Palmeira, R. de Cabo, J. A. Baur and D. A. Sinclair, SIRT1 is required for AMPK activation and the beneficial effects of resveratrol on mitochondrial function, *Cell Metab.*, 2012, **15**, 675–690.
- 27 S. Enerback, A. Jacobsson, E. M. Simpson, C. Guerra, H. Yamashita, M. E. Harper and L. P. Kozak, Mice lacking mitochondrial uncoupling protein are cold-sensitive but not obese, *Nature*, 1997, **387**, 90–94.
- 28 P. J. Antonellis, B. A. Droz, R. Cosgrove, L. S. O'Farrell, T. Coskun, J. W. Perfield 2nd, S. Bauer, M. Wade, T. E. Chouinard, J. T. Brozinick, A. C. Adams and R. J. Samms, The anti-obesity effect of FGF19 does not require UCP1-dependent thermogenesis, *Mol. Metab.*, 2019, **30**, 131–139.
- 29 I. H. N. Luijten, K. Brooks, N. Boulet, I. G. Shabalina, A. Jaiprakash, B. Carlsson, A. W. Fischer, B. Cannon and J. Nedergaard, Glucocorticoid-Induced Obesity Develops Independently of UCP1, *Cell Rep.*, 2019, **27**, 1686–1698.
- 30 H. M. Feldmann, V. Golozoubova, B. Cannon and J. Nedergaard, UCP1 ablation induces obesity and abolishes diet-induced thermogenesis in mice exempt from thermal stress by living at thermoneutrality, *Cell Metab.*, 2009, **9**, 203–209.
- 31 N. Pfeiffer, C. Desmarchelier, M. Blaut, H. Daniel, D. Haller and T. Clavel, Acetatifactor muris gen. nov., sp. nov., a novel bacterium isolated from the intestine of an obese mouse, *Arch. Microbiol.*, 2012, **194**, 901–907.
- 32 J. M. Ridlon, D.-J. Kang and P. B. Hylemon, Bile salt biotransformations by human intestinal bacteria, *J. Lipid Res.*, 2006, **47**, 241–259.
- 33 P. D. Cani, R. Bibiloni, C. Knauf, A. Waget, A. M. Neyrinck, N. M. Delzenne and R. Burcelin, Changes in gut microbiota control metabolic endotoxemia-induced inflammation in high-fat diet-induced obesity and diabetes in mice, *Diabetes*, 2008, **57**, 1470–1481.
- 34 S. Fang, J. M. Suh, S. M. Reilly, E. Yu, O. Osborn, D. Lackey, E. Yoshihara, A. Perino, S. Jacinto, Y. Lukasheva, A. R. Atkins, A. Khvat, B. Schnabl, R. T. Yu, D. A. Brenner, S. Coulter, C. Liddle, K. Schoonjans, J. M. Olefsky, A. R. Saltiel, M. Downes and R. M. Evans, Intestinal FXR agonism promotes adipose tissue browning and reduces obesity and insulin resistance, *Nat. Med.*, 2015, **21**, 159–165.
- 35 J. Y. Chiang, Recent advances in understanding bile acid homeostasis, *F1000Research*, 2017, **6**, 2029.
- 36 L. A. Velazquez-Villegas, A. Perino, V. Lemos, M. Zietak, M. Nomura, T. W. H. Pols and K. Schoonjans, TGR5 signalling promotes mitochondrial fission and beige remodelling of white adipose tissue, *Nat. Commun.*, 2018, **9**, 245.
- 37 J. Martel, D. M. Ojcius, C. J. Chang, C. S. Lin, C. C. Lu, Y. F. Ko, S. F. Tseng, H. C. Lai and J. D. Young, Anti-obesogenic and antidiabetic effects of plants and mushrooms, *Nat. Rev. Endocrinol.*, 2017, **13**, 149–160.
- 38 J. Martel, D. M. Ojcius, Y. F. Ko and J. D. Young, Phytochemicals as Prebiotics and Biological Stress Inducers, *Trends Biochem. Sci.*, 2020, **45**, 462–471.
- 39 L. H. Quan, C. Zhang, M. Dong, J. Jiang, H. Xu, C. Yan, X. Liu, H. Zhou, H. Zhang, L. Chen, F. L. Zhong, Z. B. Luo, S. M. Lam, G. Shui, D. Li and W. Jin, Myristoleic acid produced by enterococci reduces obesity through brown adipose tissue activation, *Gut*, 2020, **69**, 1239–1247.
- 40 Y. Yang, X. Wu, Z. Wei, Y. Dou, D. Zhao, T. Wang, D. Bian, B. Tong, Y. Xia, Y. Xia and Y. Dai, Oral curcumin has anti-arthritis efficacy through somatostatin generation via cAMP/PKA and Ca(2+)/CaMKII signaling pathways in the small intestine, *Pharmacol. Res.*, 2015, **95–96**, 71–81.
- 41 F. Yang, X. Tang, L. Ding, Y. Zhou, Q. Yang, J. Gong, G. Wang, Z. Wang and L. Yang, Curcumin protects ANIT-induced cholestasis through signaling pathway of FXR-regulated bile acid and inflammation, *Sci. Rep.*, 2016, **6**, 33052.
- 42 W. Feng, H. Wang, P. Zhang, C. Gao, J. Tao, Z. Ge, D. Zhu and Y. Bi, Modulation of gut microbiota contributes to curcumin-mediated attenuation of hepatic steatosis in rats, *Biochim. Biophys. Acta, Gen. Subj.*, 2017, **1861**, 1801–1812.
- 43 A. Worthmann, C. John, M. C. Ruhlemann, M. Baguhl, F. A. Heinsen, N. Schaltenberg, M. Heine, C. Schlein, I. Evangelakos, C. Mineo, M. Fischer, M. Dandri, C. Kremoser, L. Scheja, A. Franke, P. W. Shaul and J. Heeren, Cold-induced conversion of cholesterol to bile acids in mice shapes the gut microbiome and promotes adaptive thermogenesis, *Nat. Med.*, 2017, **23**, 839–849.
- 44 L. Sun, Y. Pang, X. Wang, Q. Wu, H. Liu, B. Liu, G. Liu, M. Ye, W. Kong and C. Jiang, Ablation of gut microbiota alleviates obesity-induced hepatic steatosis and glucose intolerance by modulating bile acid metabolism in hamsters, *Acta Pharm. Sin. B*, 2019, **9**, 702–710.
- 45 X. Han, J. Guo, M. Yin, Y. Liu, Y. You, J. Zhan and W. Huang, Grape Extract Activates Brown Adipose Tissue Through Pathway Involving the Regulation of Gut Microbiota and Bile Acid, *Mol. Nutr. Food Res.*, 2020, **64**, e2000149.
- 46 E. Somm, H. Henry, S. J. Bruce, S. Aeby, M. Rosikiewicz, G. P. Sykiotis, M. Asrih, F. R. Jornayvaz, P. D. Denechaud, U. Albrecht, M. Mohammadi, A. Dwyer, J. S. Acierno Jr., K. Schoonjans, L. Fajas, G. Greub and N. Pitteloud, beta-

- Klotho deficiency protects against obesity through a cross-talk between liver, microbiota, and brown adipose tissue, *JCI Insight*, 2017, 2(8), e91809.
- 47 T. Q. de Aguiar Vallim, E. J. Tarling and P. A. Edwards, Pleiotropic roles of bile acids in metabolism, *Cell Metab.*, 2013, 17, 657–669.
- 48 P. Xu, J. Wang, F. Hong, S. Wang, X. Jin, T. Xue, L. Jia and Y. Zhai, Melatonin prevents obesity through modulation of gut microbiota in mice, *J. Pineal Res.*, 2017, 62(4), DOI: 10.1111/jpi.12399.
- 49 J. Liu, Y. Li, P. Yang, J. Wan, Q. Chang, T. T. Y. Wang, W. Lu, Y. Zhang, Q. Wang and L. L. Yu, Gypenosides Reduced the Risk of Overweight and Insulin Resistance in C57BL/6J Mice through Modulating Adipose Thermogenesis and Gut Microbiota, *J. Agric. Food Chem.*, 2017, 65, 9237–9246.
- 50 J. F. Pierre, K. B. Martinez, H. Ye, A. Nadimpalli, T. C. Morton, J. Yang, Q. Wang, N. Patno, E. B. Chang and D. P. Yin, Activation of bile acid signaling improves metabolic phenotypes in high-fat diet-induced obese mice, *Am. J. Physiol.: Gastrointest. Liver Physiol.*, 2016, 311, G286–G304.
- 51 F. F. Anhe, R. T. Nachbar, T. V. Varin, J. Trottier, S. Dudonne, M. Le Barz, P. Feutry, G. Pilon, O. Barbier, Y. Desjardins, D. Roy and A. Marette, Treatment with camu camu (*Myrciaria dubia*) prevents obesity by altering the gut microbiota and increasing energy expenditure in diet-induced obese mice, *Gut*, 2019, 68, 453–464.